Websites

http://www.liiscience.org
http://www.vbt.uni-karlsruhe.de/specialtopic/2ndLIIWS2006/Internetauftritt1.htm
http://liiscience.org/05_workshop_home

Contact

bockhorn@ict.uni-karlsruhe.de
charwath@ict.uni-karlsruhe.de
suntz@ict.uni-karlsruhe.de

Organizers

Henning Bockhorn (TCP, Universität Karlsruhe)
Rainer Suntz (TCP, Universität Karlsruhe)
Per-Erik Bengtsson (Lund Institute of Technology, Lund)
Klaus-Peter Geigle (DLR, Stuttgart)
Boris Kock (IVG, Universität Duisburg-Essen)
Fengshan Liu (NRC Canada, Ottawa)
Hope Michelsen (Sandia National Laboratories, Livermore)
Christof Schulz (IVG, Universität Duisburg-Essen)
Greg Smallwood (NRC Canada, Ottawa)
Stefan Will (TT, Universität Bremen)
Giorgio Zizak (CNR-IENI, Milano)

Co-organized with

CRC 606 „Non-stationary Combustion“

Location

Haus der Kirche - Evangelische Akademie Baden
Dobler Str. 51,
76332 Bad Herrenalb

Tel: ++49 (0)7083/928- 0
Fax: ++49 (0)7083/928-601
haus@ev-akademie-baden.de

Registration

Registration is possible during the get together on Wednesday (17:00, Haus der Kirche, see below) and on Thursday morning at 8:00 to 10:00.

Welcome get-together

On Wednesday, August 2 an informal get together will be offered in Haus der Kirche starting with the dinner from 17:30.

Conference dinner

The conference dinner will be held on Thursday night at Schloss Eberstein. The bus will leave at Haus der Kirche at 19:00. After the dinner bus transfer to the Haus der Kirche will be provided.

SCHLOSS EBERSTEIN
RESTAURANT & HOTEL

Exhibition

Please visit the exhibition of our Sponsors LaVision, Quantel, Innolas and Radiant Dyes.

Sponsors

We acknowledge the financial support of:

Deutsche Forschungsgemeinschaft DFG

pco. imaging

COHERENT

Quantel

Innovative INNOLAS Lasertechnologie

LAVISION WE COUNT ON PHOTONS

Radiant Dyes Laser Accessoires GmbH

Program

Wednesday, Aug. 2: Conference

17:30 **Informal get together**

Thursday, Aug. 3: Conference and Workshop (Part I)

8:30 **Welcome**

Modeling

8:50 **Theoretical considerations in modeling LII at low pressures**
F. Liu, K. J. Daun, G. J. Smallwood
National Research Council of Canada, Ottawa, Canada

9:10 **Inverse analysis of time-resolved LII data**
K. J. Daun[1], F. Liu[1], G. J. Smallwood[1], B. J. Stagg[2], and D. R. Snelling[1]
[1]National Research Council of Canada, Ottawa, ON, Canada, K1A 0R6
[2]Columbian Chemicals Company, Marietta, GA, USA

9:30 **Heat conduction from spherical nano-particles**
F. Liu, K. J. Daun, G. J. Smallwood, and D. R. Snelling
National Research Council of Canada, Ottawa, Canada

Special LII Techniques and Combined Techniques

9:50 **Absorption correction of two-color LII-signals**
F. Migliorini, S. De Iuliis, F. Cignoli, G. Zizak
CNR-IENI, Istituto per l'Energetica e le Interfasi, Milano, Italy

10:10 **Coffee break**

10:40 **Longer laser pulses for practical LII**
J. D. Black
Strategic Research Centre, Rolls-Royce plc, Derby, UK

11:00 **TR-LII and PMS particle sizing applied to soot particles synthesized in a low-pressure flame reactor**
B. Tribalet, B.F. Kock, P. Ifeacho, P. Roth, C. Schulz
IVG, Universität Duisburg-Essen, Germany

11:20 **Time-resolved LII in comparison with mass-spectrometry measurements in a premixed ethylene/air flame**
R. Stirn, K.P. Geigle, W. Meier, T. Gonzalez-Baquet, H.H. Grotheer, M. Aigner
Institute of Combustion Technology, German Aerospace Center (DLR), Stuttgart

11:40 **Temperature measurements for LII evaluation in non-premixed flames – comparison between emission spectroscopy and CARS**
M. Wendler, G. Guevara, M.C. Weikl, R. Sommer, F. Beyrau, T. Seeger and A. Leipertz
Lehrstuhl für Technische Thermodynamik, Universität Erlangen-Nürnberg, Germany

12:00 **Lunch**

Pressure Effects

13:10 **Pressure effects on LII signals**
A. Boiarciuc[1], F. Foucher[1], C. Mounaïm-Rousselle
Laboratoire de Mécanique et d'Energétique, University of Orléans, France

13:30 **Effect of pressure on thermal accommodation coefficient**
B.J. Stagg
Columbian Chemicals Company Marietta, GA, USA

Applications

13:50 **Laser induced incandescence for measuring soot particle emission from aero-gas turbines**
J. Delhay[1], P. Desgroux[1], E. Therssen[1], John Black[2]
[1]PC2A, UMR-CNRS 8522, Université des Sciences et Technologies de Lille, Villeneuve D'ascq, France
[2] Strategic Research Centre, Rolls Royce plc, Derby, UK

14:10 **Two-color time-resolved LII study of iron oxide nanoparticle formation in a premixed flat low pressure flame**
H. Dörr, H. Bockhorn and R. Suntz
Institute for Chemical Technology and Polymer Chemistry, University of Karlsruhe (TH), Germany

Poster Session (with Coffee break)

14:30 **Poster Session**

P01 **In-cylinder particulate sizing with combined TR-LII/2C pyrometry**
B. Bougie[1,2], L.C. Ganippa[1,3], A.P. van Vliet[1], W.L. Meerts[1], N.J. Dam[1], J.J. ter Meulen[1]
[1]Applied Molecular Physics, Institute for Molecules and Materials, Radboud University Nijmegen, The Netherlands
[2]Current address: Multi-Scale Physics Delft University of Technology, Delft, The Netherlands
[3]Current address: School of Engineering and Design, Brunel University, London, UK

P02 **Pressure effect on the determination of particle-size distributions in a sooting methane diffusion flame**
M. Charwath, R. Suntz, H. Bockhorn
Institute for Chemical Technology and Polymer Chemistry, University of Karlsruhe (TH), Germany

P03 **Measuring accommodation coefficients using laser-induced incandescence**
K. J. Daun, G. J. Smallwood, F. Liu, and D. R. Snelling
National Research Council of Canada, Ottawa, Canada

P04 **Comparison of TR-LII sizing for pure carbon and hydrogen-containing carbon particles**
A. Eremin[1], M. Falchenko[1], E. Gurentsov[1], B. Kock[2], R. Starke[2], C. Schulz[2]
[1]Institute for High Energy Density RAS, Moscow, Russia
[2]IVG, Universität Duisburg-Essen, Duisburg, Germany

P05 **LII in a high vacuum and up date and LII in carbon black from a particle generator**
V. Beyer[1] and D. A. Greenhalgh[1], D. Clavel[2], K. Daun[2], F. Liu[2], B. Sawchuck[2], G. Smallwood[2], D. Snelling[2] and K. Thomson[2]
[1]School of Engineering Cranfield University
[2]National Research Council of Canada, Ottawa, Canada

P06 **Particle size measurements with two color TIRE-LII**
R. Hadef[1], R. Stirn[2], KP. Geigle[2], M. Aigner[2]
[1]Institut de Génie Mécanique, Université Larbi Ben M'Hidi, Oum El Bouaghi, Algérie
[2]Institut für Verbrennungstechnik, DLR, Stuttgart, Germany

P07 **A web-based interface for modeling laser-induced incandescence (LIISim)**
M. Hofmann, B.F. Kock, C. Schulz
IVG, Universität Duisburg-Essen, Duisburg, Germany

P08 **Effects of soot absorption and scattering on LII intensities in a laminar coflow ethylene/air diffusion flame**
F. Liu, K. A. Thomson, G. J. Smallwood
Institute for Chemical Process and Environmental Technology, National Research Council, Canada

P09 **Time-resolved laser-induced incandescence (TIRE-LII) coupled with spectral emission measurements for particle sizing in high-pressure diesel combustion environments**
R. Ryser, T. Gerber, T. Dreier
Paul Scherrer Institute, Department of General Energy, Reaction Analysis Group, Villigen PSI, Switzerland

P10 **Prompt heat transfer in near-sublimation regime LII**
F. Liu, K. J. Daun, G. J. Smallwood, and D. R. Snelling
National Research Council of Canada, Ottawa, Canada

P11 **Design optimization for high sensitivity two-color LII**
G. J. Smallwood
Institute for Chemical Process and Environmental Technology, National Research Council, Canada

P12 **Absolute Intensity calibration of LII detectors**
K. A. Thomson, D. R. Snelling, G. J. Smallwood
Institute for Chemical Process and Environmental Technology, National Research Council, Canada

18:15 **End of Poster Session**

19:00 **Bus transfer to Conference Dinner at Schloss Eberstein (return ~ 23:00)**

Friday, Aug. 4: Workshop

8:30 **Modeling of the LII-process**

Boris Kock, IVG, Universität Duisburg-Essen, Germany
Fengshan Liu, National Research Council, Canada
Hope Michelsen, CRF, Sandia National Laboratories, Livermore, CA, US

Comparison of different models (reference flames) – particle heating and cooling mechanisms – temperature dependence of heat capacity – different Knudsen regimes – influence of particles size distribution and agglomeration on LII – consideration of radial and temporal distribution of the laser beam – influence of pressure and ambient gas temperature – material properties

10:30 **Coffee break**

11:00 **Experimental**

Klaus-Peter Geigle, VT, DLR Stuttgart, Germany
Greg Smallwood, National Research Council, Canada

Excitation wavelength – radial and temporal energy distribution – devices for homogenisation of laser fluence – one- or two-dimensional detection – detection systems – detection wavelength – potential interferences – detection at high-pressure and/or low ambient gas temperatures (detectors response function, (de)convolution of the signal) – influence of laser fluence (particle morphology, aggregate structure) – two color techniques – mass spectrometry: fragments evaporating from the particle surface – Pump and probe experiments – estimation of accommodation coefficient from shock-tube experiments – photolytically generated soot particles by decomposition of C_3O_2 *– LII at high temporal resolution – single particle LII*

12:00 **Lunch**

13:10 **Experimental (continuation)**

14:10 **Signal evaluation**

Thomas Dreier, CRL, Paul Scherrer Institut, Switzerland
Giorgio Zizak, CNR-IENI, Italy

Determination of particle size distribution (fitting of measured curves or Fredholm equation) – influence of particle shape (primary particles and agglomerates) – calibration

15:10 **Coffee break**

15:40 **Signal evaluation (continuation)**

16:40 **LII of non-soot particles**

Per-Erik Bengtsson, LIT-CP, Sweden
Stefan Will TT, Universität Bremen, Germany

Particles accessible for LII – evaporation temperature – particle constants (absorption coefficients, accommodation coefficients, etc.) – limitations – modification of the model – additional physical effects

18:00 **Summary and conclusions of the workshop, hot topics and location of the next workshop**

19:00 **Dinner**

Poster Session (continuation)

20:15 **Poster Session**

Theoretical considerations in modeling LII at low pressures

F. Liu*, K. J. Daun, G. J. Smallwood
Institute for Chemical Process and Environmental Technology
National Research Council, Canada

This study presents some fundamental considerations in modeling LII at low-pressures and identifies conditions under which particle radiation heat loss dominants over sublimation and conduction.

Introduction

Low-pressure LII has received some attention in the literature. The rationale of conducting LII experiments in this regime is to minimize particle heat conduction loss and to extend the signal lifetime. If the particle temperature is sufficiently low to neglect sublimation heat loss, particle cooling occurs primarily through radiation and consequently low-pressure LII can be used to study radiative properties of nano-sized particles.

Several incorrect expressions for particle radiation heat loss rate exist in the LII literature, however, which have led some authors to erroneously claim that near-vacuum LII can be used as a nanoparticle sizing technique. One of the main objectives of this study is to establish the correct expression for radiation heat loss rate from a spherical particle. We also investigate the error inherent in using the Rayleigh approximation to calculate particle laser energy absorption and the implication for two-color LII. Conditions under which particle radiation heat loss is dominant are identified in terms of particle temperature, pressure, and particle diameter, and a brief discussion is given on absorption and emission by aggregated particles.

LII Model and Theoretical Considerations

We employ the conventional single-particle based LII model given by

$$\frac{\pi d_p^3}{6}\rho_s c_s \frac{dT}{dt} = Q_{abs}\pi d_p^2 F_0 q(t) + \dot{q}_{rad} + \dot{q}_{cond} + \dot{q}_{sub} \quad (1)$$

$$\frac{dM}{dt} = \frac{\rho_s \pi d_p^2}{2}\frac{dd_p}{dt} = -\pi d_p^2\, \beta\, p_v \sqrt{\frac{M_v}{2\pi RT}}. \quad (2)$$

Radiant loss rate from a spherical particle is written as

$$q_{rad} = -\pi d_p^2 \int_0^\infty Q_{abs} E_{b,\lambda}\, d\lambda = -\pi d_p^2 \int_0^\infty \varepsilon_\lambda\left(d_p\right) E_{b,\lambda}\, d\lambda. \quad (3)$$

The particle absorption efficiency, Q_{abs}, obtained using both Rayleigh and Mie theories over size parameters relevant to LII is plotted in Fig. 1. Rayleigh theory underestimates Q_{abs} for size parameters greater than 0.15.

Figure 2 shows the conditions under which the ratios q_{rad}/q_{cond} and q_{rad}/q_{sub} are greater than 10 for a particle of 30 nm in diameter. For radiation heat loss to dominate, the particle temperature and gas pressure must be below 2760 K and 3×10^{-4} atm respectively.

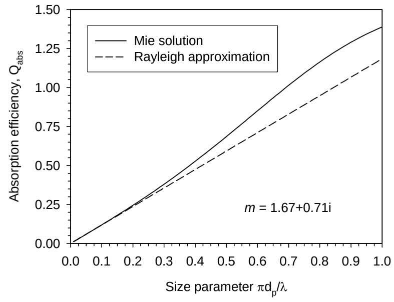

Fig.1: Absorption efficiencies calculated using Rayleigh and Mie theories.

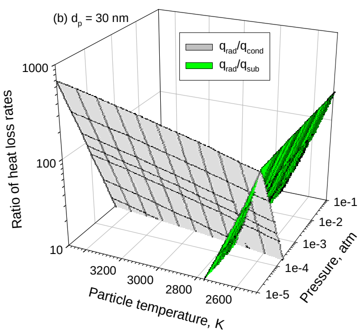

Fig.2 Variation of q_{rad}/q_{cond} and q_{rad}/q_{sub} with particle temperature and pressure for d_p = 30 nm.

The effect of using the Rayleigh approximation when predicting the effective temperature, T_e, of a polydisperse particle ensemble is also investigated. Rayleigh approximation could predict significantly lower peak particle temperature, especially when the green laser (λ = 532 nm) is used. The decay of T_e^{-4} under conditions where radiation heat loss is dominant is proportional to $\overline{E}(m)$, the mean particle absorption function over the visible and IR, for particles within the Raleigh regime.

Conclusions

Using the Rayleigh approximation can potentially induce considerable error in LII modeling for both laser energy absorption and the particle temperature analysis using two-color LII. Near-vacuum LII experiments can only be used to determine the mean value of E(m) provided that the particles are in the Rayleigh limit. Only under conditions of sufficiently low pressure and sufficiently low particle temperature radiation heat loss is the dominant particle cooling mechanism.

* Corresponding author: fengshan.liu@nrc-cnrc.gc.ca

International Discussion Meeting and Workshop 2006: Laser-induced Incandescence, Quantitative interpretation, modelling, application

Inverse analysis of time-resolved LII data

K. J. Daun[1*], F. Liu[1], G. J. Smallwood[1], B. J. Stagg[2], and D. R. Snelling[1]
[1]National Research Council of Canada, Ottawa, ON, Canada
[2]Columbian Chemicals Company, West Oak Commons Ct., Marietta, GA, USA

This study reviews techniques for recovering aerosol particle size distributions from time-resolved laser-induced incandescence data in the context of solving a mathematically ill-posed inverse problem.

Introduction

Time-resolved LII has recently evolved into a tool for evaluating particle size distributions in aerosols. Since larger particles cool slower than smaller particles the size distribution can be recovered from the observed monochromatic incandescence or effective temperature decays.

This involves solving a mathematically ill-posed inverse problem, which is complicated by the fact that ill-posed problems may not have a solution, have multiple solutions, or have a solution that is sensitive to perturbations to the problem. Although solution existence is guaranteed in this case, uniqueness and stability are not, which is of particular concern in LII experiments since physical parameters are not known with a high-degree of certainty and experimental data often contains substantial shot-noise. Because of these difficulties, special explicit and implicit techniques must be used to solve ill-posed inverse problems.

Explicit Methods

Explicit methods solve the mathematically ill-posed governing equations directly. In this problem, the monochromatic incandescence at any instant, $J_\lambda(t)$, is governed by a Volterra integral equation of the first-kind,

$$J_\lambda(t) = C_\lambda \int_0^\infty f(d_p) K_\lambda(t, d_p)\, d d_p, \tag{1}$$

where C_λ is a constant, $f(d_p)$ is the unknown particle size distribution, and $K_\lambda(t, d_p)$ is the radiation emitted by particles of diameter d_p at time t and wavelength λ. Explicit methods transform ill-posed integral equations into ill-conditioned matrix equations, **Ax** = **b**, which are then solved using regularization methods. Roth and Filippov [1] used iterative regularization to solve Eq. (1) for $f(d_p)$.

Implicit Methods

Implicit methods work on the well-posed forward problem, which in this case is to determine the $J_\lambda(t)$ or the effective temperature, $T_e(t)$ that corresponds to a particular $f(d_p)$. Different size distributions are then substituted into the governing equations until the modeled $J_\lambda(t)$ or $T_e(t)$ matches the experimentally-observed values. This is most efficiently done by casting the problem as a least-squares minimization problem,

$$\min_x [F(\mathbf{x})] = \min_x \left[\left\| \mathbf{f}^{\exp} - \mathbf{f}^{\mathrm{mod}}(\mathbf{x}) \right\|_2^2 \right], \tag{2}$$

where **x** specifies $f(d_p)$ (which is usually log-normal) and $\mathbf{f}^{\exp}$ and $\mathbf{f}^{\mathrm{mod}}(\mathbf{x})$ contain experimentally-observed and modeled data, respectively. F(**x**) is then minimized using nonlinear programming; the minimizer **x*** specifies the particle size distribution that best describes the experimentally-observed results. This approach has been used [2-5] to find $f(d_p)$ using $J_\lambda(t)$ or $T_e(t)$. Liu et al. [5] transform this problem into an easier-to-solve univariate minimization problem.

Although implicit methods work on the well-posed forward problem, the ill-posedness of the inverse problem is manifested in the topography of F(**x**), shown in Fig. 1. The valley surrounding $\mathbf{x}^*$ corresponds to particle size distributions that nearly produce the experimentally-observed data. Diamonds show solutions found using data contaminated with shot noise. Accordingly, care must be taken to select a method that is insensitive to uncertainties in the parameters and experimental error.

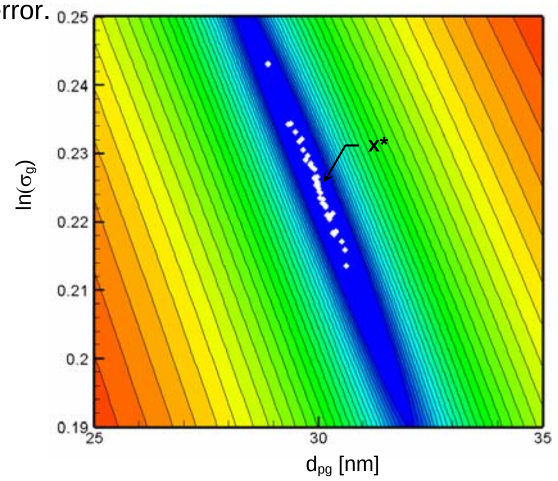

Fig. 1: Plot of F(x), showing solutions obtained using perturbed incandescence data.

[1] P. Roth, A. V. Filippov,J. Aerosol Sci. 27, 95-104 (1996).
[2] T. Lehre, B. Jungfleisch, R. Suntz, H. Bockhorn, App. Opt. 42, 2021-2029 (2003).
[3] S. A. Kuhlmann, J. Schumacher, J. Reimann, S. Will, PARTEC, Nuremburg, Mar. 16-18 (2004)
[4] S. Dankers, A. Leipertz, App. Opt. 43 3726-3730 (2004)
[5] F. Liu, B. J. Stagg, D. R. Snelling, G. J. Smallwood, IJHMT, 49, 777-788 (2006).

* Corresponding author: kyle.daun@nrc-cnrc.gc.ca
International Discussion Meeting and Workshop 2006: Laser-induced Incandescence, Quantitative interpretation, modelling, application

Heat conduction from spherical nano-particles

F. Liu*, K. J. Daun, G. J. Smallwood, and D. R. Snelling
National Research Council of Canada, Ottawa, Canada

This study describes the physics of conduction heat transfer from nano-sized spherical particles and interpolation techniques used to calculate heat transfer in the transition regime. The accuracy of these techniques is evaluated by comparing their results with those obtained by direct Monte Carlo simulation.

Introduction

An accurate model of conduction heat transfer from a small sphere immersed in a gas and an understanding of the underlying physics are essential when analyzing data from time-resolved laser-induced incandescence experiments. This work summarizes recent reviews [1, 2] of this problem.

The governing physics is specified by the Knudsen number, $Kn = \lambda_{MFP}/a$. If Kn is very large, heat transfer occurs in the free-molecular regime. In this regime molecules travel between the particle and the equilibrium gas without colliding, and the heat transfer rate is given by

$$q_{FMR}(Kn) = \alpha_T \, \pi a^2 \frac{P_g \bar{c}}{2} \frac{\gamma^* + 1}{\gamma^* - 1}\left(\frac{T_p}{T_g} - 1\right), \quad (1)$$

where α_T is the thermal accommodation coefficient, $\bar{c}$ is a characteristic molecular speed, and γ^* is the temperature-averaged adiabatic gas constant. The heat transfer rate increases with increasing molecular number density and is thus proportional to P_g and Kn^{-1}.

If Kn is very small heat transfer occurs in the continuum regime,

$$q_c = 4\pi a \bar{k}_c \left(T_p - T_g\right), \quad (2)$$

where $\bar{k}_c$ is the temperature-averaged thermal conductivity. In this regime q_c is independent of pressure and Kn since increasing P_g increases the molecular number density but decreases the distance between intermolecular collisions.

If Kn is neither small nor large conduction occurs in the transition regime. The physics of this regime is dominated by a collisionless layer surrounding the particle that causes a temperature jump at the gas-surface interface. Since the Boltzmann equation is analytically intractable in this regime, heat transfer is instead estimated using schemes that interpolate between q_{FMR} and q_c.

Transition-Regime Interpolation Schemes

Transition-regime interpolation schemes are categorized as being either simple-interpolative, diffusion-approximation, or boundary-sphere methods. The most popular simple-interpolative technique is by McCoy and Cha [3], who defined an overall collision frequency as the sum of intermolecular and molecule-wall collision frequencies. Substituting this into the Chapman-Enskog approximation for k_c results in

$$\frac{q_{trans}(Kn)}{q_c} = \frac{1}{1 + G\,Kn}, \quad (3)$$

where G is a geometry-specific parameter.

Diffusion-approximation (DA) techniques estimate q_{trans} using Eq. (2) but adjust T_P to account for the temperature-jump specified by the slip parameter ξ. After rearranging, it can be shown that

$$\frac{q_{trans}(Kn)}{q_c} = \frac{1}{1 + \xi\,Kn}, \quad (4)$$

where ξ is given by Loyalka [4].

Boundary-sphere (BS) methods work by finding the unknown temperature at the interface of the collisionless layer and the continuum gas, T_δ, by solving $q_{FMR}(T_p, T_\delta) = q_c(T_\delta, T_g)$. Although this is traditionally done analytically, a numerical technique [2] has recently been proposed that accounts for temperature-dependent gas properties.

Figure 1 shows solutions obtained using the interpolation schemes and by direct Monte Carlo simulation. Note that temperature-dependent gas properties must be considered when analyzing LII data, and the Loyalka DA model only applies to monatomic gases. The BS method of [2] is the most accurate scheme for analyzing LII data.

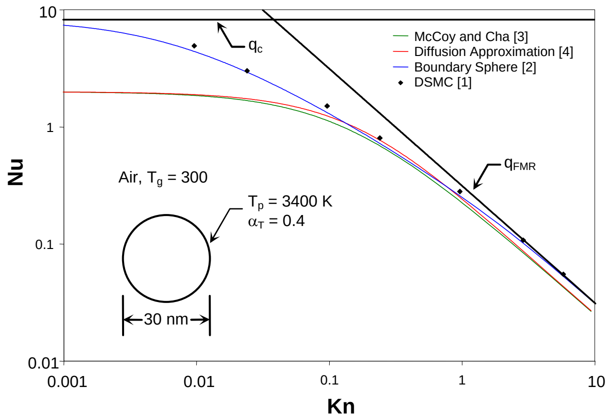

Fig. 1: Transition-Regime Interpolation Schemes and DSMC Results.

[1] F. Liu, K. J. Daun, D. R. Snelling, G. J. Smallwood, App. Phys. B. 83, 3, 355-382 (2006).

[2] A. V. Filippov, D. E. Rosner, IJHMT 43, 127-138 (2000).

[3] B. J. McCoy, C. Y. Cha, Chem. Eng. Sci. 29, 381-388 (1974).

[4] S. K. Loyalka, Prog. Nuc. Energy 12, 1-56 (1983).

* Corresponding author: Fengshan.liu@nrc-cnrc.gc.ca
International Discussion Meeting and Workshop 2006: Laser-induced Incandescence, Quantitative interpretation, modelling, application

Absorption correction of two-color LII-signals

F. Migliorini, S. De Iuliis, F. Cignoli, G. Zizak*
CNR-IENI, Istituto per l'Energetica e le Interfasi, Milano, Italy

In this work we present a numerical iterative procedure for the evaluation of the effect of signal absorption in two-color laser-induced incandescence (2C-LII) measurements. The correction process is applied to experimental results, previously published by our group, in an axisymmetric diffusion flame. We have studied the influence of signal trapping on peak soot temperature and on soot volume fraction determination. The influence was found to be minimal for the investigated flame. Some numerical tests were also performed in order to investigate the effects of soot concentration, flame size and soot refractive index on the magnitude of the corrections due to signal absorption.

Introduction

Two-color LII technique is proposed for absolute soot volume fraction measurements without the need for a calibration procedure performed in an environment of known soot concentration. Absorption corrections, as obtained trough an iterative numerical procedure, are applied in order to evaluate their influence on peak temperature and, therefore, on soot volume fraction measurements. This work shows that 2C-LII technique present an intrinsic stability in the determination of soot volume fraction, even in the case of soot load and refractive index variations.

Numerical Procedure and Results

The procedure for absorption correction is essentially based on an iterative process[1]. It has been applied to raw LII data taken on a laminar ethylene diffusion flame and reported in a previous publication[2]. The correction for absorption of LII signals at two wavelengths takes into account the soot amount in the region between the detection optics and the origin of the LII signals. The iterative procedure is quite simple. The original measured signals at two wavelengths are elaborated through an Abel inversion procedure in order to obtain radial LII emission profiles. From the ratio of the two signals the radial profiles of peak soot temperature and volume fraction are calculated. This last is utilized in the calculation of the absorption corrected signals. The entire procedure is repeated until the difference in soot volume fraction is minimized. Because the absorption at the two wavelengths is different, the result of the procedure is to increase the "true" corrected temperature (about 50-70 K) with the consequent decrease of volume fraction even though signals are higher because of absorption corrections. The application of the 2C-LII technique, with the competitive effects of the correction for the two signals allows to obtain soot volume fraction values that weakly depend on absorption corrections.

In order to gain a better view of different aspects of signal trapping, some numerical simulations have been also performed. These tests were carried out by changing the soot amount, trough variation of the LII-signal intensities and flame size, by multiplying them by factors 2, 5 and 10. The trend is the same as previously observed. Only for the unreal largest correction (factor 10) the peak temperature profile is heavily distorted and, as a consequence, also the soot volume fraction profile is much different from the original one.

Another interesting test was performed to analyze the role of soot refractive index. Soot temperature depends on the ratio of the values of E(m) calculated at the two measuring wavelengths. The choice of the refractive index is still a debated issue and comparison of soot volume fraction results must take this into account. In general we use the data of Chang and Charalampopoulos[3], involving a slight decrease of E(m) with wavelength. In this test we used the data of Krishnan et alii[4] which present an opposite slope. The results of the calculations show that the peak temperatures reach values around 4500-4600 K. This influences the soot concentration values that are half of what was previously measured and in disagreement with extinction measurements using the same set of refractive index. Nevertheless the absorption correction is negligible even in this case.

Conclusions

The 2C-LII technique has been shown to be rather insensitive to absorption corrections. Considering that it can also give absolute soot concentration measurements the 2C-LII technique results to be a very powerful tool for soot diagnostics.

[1] M.Y. Choi, K.A. Jensen, Combust,. Flame, 112, 485-491 (1998).
[2] S. De Iuliis, F. Cignoli, G. Zizak, Appl. Opt. 44, 7414-7423 (2005).
[3] H. Chang, T.T. Charalampopoulos, Proc. R. Soc. London, Ser. A 430, 577-591 (1990).
[4] S.S. Krishnan, K.C. Lin, G.M. Faeth, J. Heat Transfer, 122, 517-524 (2000).

*Corresponding author: zizak@ieni.cnr.it

Longer laser pulses for practical LII

J. D. Black*
Strategic Research Centre
Rolls-Royce plc, Derby, UK

To date nearly all LII is carried out using Q-switched, flashlamp pumped Nd/YAG lasers with pulse lengths ~10 ns. Although these lasers are well developed and readily available for use in the laboratory and in commercial instruments, they are bulky, inefficient and often the most costly part of an LII system. Cheaper, more compact lasers are becoming available, but very few are able to match the 10 ns pulse length and >100 mJ/pulse capability of Nd/YAG.

Background

The first published LII experiment [1] used a CO_2 TEA laser with microsecond pulses and some early work by Eckbreth [2] used a flashlamp pumped dye laser. However, since the expansion of the use of LII for combustion studies in the mid 1980s, the standard source has become the Q-switched, flashlamp pumped Nd/YAG operating at either 1064 or 532 nm. A picosecond lasers has been used to study the fundamental LII process [3], but very little attention has been given to the possibility of using longer pulse lasers.

Lasers for Practical Applications of LII

While the most common use of LII is the study of soot distribution in laboratory flames, there are commercial LII instruments in use for vehicle emission and atmospheric monitoring and at least three systems worldwide have been used to make in-situ measurements in aero-engine exhausts. The vehicle exhaust and atmospheric system perform LII on sampled gas within a light tight enclosure and so are not subject to laser safety constraints. However, the Nd/YAG laser is usually the largest, heaviest and most expensive part of these systems. It is very difficult to sample gas from an aero-engine exhaust and a major advantage of LII is that it can be applied in-situ. However, this involves irradiating the exhaust plume with a Class 4 laser, often at a wavelength of 1064 nm where eye safety is most difficult, and so its use is restricted to enclosed test beds or airfields which can be closed off. Lasers producing longer pulses and operating at longer wavelength (>1500 nm) would be subject to less stringent safety restrictions and could be used for in-situ measurement in a wider range of locations.

It may also be possible to combine LII with laser absorption spectroscopy using a mid or near IR laser to measure molecular species in an exhaust.

Developments in Lasers

New types of lasers which may be suitable for LII are becoming widely used, often in non-scientific applications, for example pulsed diode lasers in the printing industry and fibre lasers for welding and cutting applications. Both these types, which are lighter and more compact than their Nd/YAG equivalents can produce pulses with energies in the 10's of millijoules and pulse lengths of a few microseconds. Experiments with a fibre laser producing 5 mJ in 10 μs pulses which have an initial spike <1 μs are planned in an engine exhaust.

Conclusions

Model predictions show an increase in LII with longer pulses [4], perhaps because there is less competition with other processes such as sublimation, though annealing and ablative processes could be quite different with longer pulses. LII with lasers producing longer pulses than standard Q-switched Nd/YAG has been a neglected area of study, which may prove very useful for the advancement of the practical application of the technique in the future.

[1] R.W. Weeks and W.W. Duley, J. Appl. Phys. 45, 4661 (1974)

[2] A.C. Eckbreth, J. Appl. Phys. 48, 4473 – 4479 (1977)

[3] H.A. Michelsen, Appl. Phys. B, 83, 443 – 448 (2006)

[4] H.A. Michelsen, personal communication

* Corresponding author: john.black@rolls-royce.com

TR-LII and PMS particle sizing applied to soot particles synthesized in a low-pressure flame reactor

B. Tribalet, B.F. Kock*, P. Ifeacho, P. Roth, C. Schulz
IVG, Universität Duisburg-Essen, Germany

Laser-induced incandescence with time-resolved detection (TR-LII) was applied for size measurements of soot nanoparticles in a low-pressure flame reactor. The results are compared with the particle sizes determined by a particle mass spectrometer (PMS).

Soot particles were synthesized in a rich $C_2H_2/O_2/Ar$ premixed flat flame in a low-pressure reactor [1,2]. The same apparatus has been used previously to synthesize nanoparticles from a large range of materials [3]. Fig. 1 schematically shows the main components of the experimental setup.

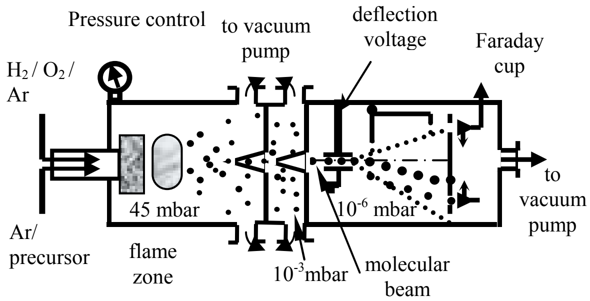

Fig. 1: Premixed flame reactor

The pressure in the reactor was maintained at 45 mbar while the inlet gas velocity was kept constant at 0.87 m/s. High soot concentration caused a bright yellow flame. The soot particle-size distribution was determined with a particle mass spectrometer (PMS) [1,2] attached to the premixed flame reactor. The residence time in the reactor can be changed by moving the burner head relative to the PMS sampling location and the LII probe volume, respectively. Depending on the residence time the mean particle diameter varied between 15 and 18 nm. The geometric standard deviation σ_g was within the range of 1.44 and 1.69. TR-LII experiments were performed simultaneously in the reactor close to the PMS sampling location. The reactor was equipped with three fused silica windows used for the incident and transmitted laser beam and for signal detection. The Nd:YAG laser for particle heating is operated at a wavelength of 1064 nm (Beam diameter: 8 mm) and has a pulse duration of 6 ns. The pulse energy was about 240 mJ for the present experiments. The detection system was arranged perpendicular to the laser beam axis and was composed of a *f* = 150 mm lens, which collected the particle radiation. A narrow band-pass filter with a center wavelength of 550 nm limits the radiation to a small spectral range. Finally, a collecting lens (*f* = 50 mm) focuses the beam onto the photo cathode of a high-speed photomultiplier with integrated amplifier (SMT MEA 1030 V8DA with HAMAMATSU R7400U-04, rise time: 0.78 ns). The signal was stored by a digital oscilloscope (TEKTRONIX TDS 3052, 500 MHz) at a sample rate of 5 Gs/s.

Results and discussion

Figure 2 shows a typical individual normalized TR-LII signal reduced for the period of particle cooling measured in the flame reactor and the best obtained fit as a function of time.

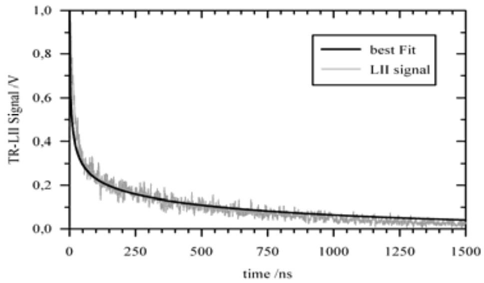

Fig. 2: Measured TR-LII raw signal

The measured signal was evaluated in terms of particle size by fitting a simulated signal curve by least-squares method. The used TR-LII model is presented in [4], while the required thermal accommodation coefficient α_T of the soot particles was assumed to be 0.23 in the present case. For further simplification it was assumed that the particles were heated up to the evaporation temperature of 3900 K. For a lognormal size distribution of the particles best fit conditions were obtained at a count mean diameter (CMD) between 17 and 20 nm and a geometric standard deviation of 1.1. These results are in good agreement with the results of the PMS-measurements. The combination of TR-LII and molecular-beam with subsequent particle-mass spectrometry in low pressure flames is a promising approach for fundamental research on the characteristics of LII of various well characterized nano-particular materials.

[1] H. Kleinwechter, C. Janzen, J. Knipping, H. Wiggers, P. Roth, J. Mat. Sci. 37, 4349-4360 (2002).
[2] V. Simanzhenkov, P. Ifeacho, H. Wiggers, J., Knipping, P. Roth, J. Nanosci. Nanotech. 4, 157-161 (2004).
[3] P. Roth, Proc. Combust. Inst. 31, (2006), in press.
[4] B.F. Kock, C. Kayan, J. Knipping, H.R. Orthner, P. Roth, Proc. Combust. Inst. 30, 1689-1697 (2005)

* Corresponding author: boris.kock@uni-due.de
International Discussion Meeting and Workshop 2006: Laser-induced Incandescence, quantitative interpretation, modelling, application

Time-resolved LII in comparison with mass spectrometry measurements in a premixed ethylene/air flame

R. Stirn*, K.P. Geigle, W. Meier, T. Gonzalez-Baquet, H.H. Grotheer, M. Aigner
Institute of Combustion Technology
German Aerospace Center (DLR), Stuttgart, Germany

The measurement of combustion generated nano- and sootparticles with sizes up to 20 nm remains a challenge as all current size measurement techniques do not cover the whole range of particle sizes. Therefore it is necessary to combine different methods. In addition it is essential to find the overlapping detectable regions for comparison of the different sizing methods.

Introduction

We have used two alternative methods, LII and photoionization mass spectrometry to obtain particle sizes under well defined experimental conditions. To this end a McKenna burner was used with an ethylene/air flame stabilized by a horizontal stainless steel plate located 21 mm above the burner surface. Measurements were carried out for equivalence ratios ranging from Φ=1.8 to 2.4. Furthermore the particle sizes have been determined as a function of the height above burner (HAB) between 6 and 16 mm. Additionally first LII measurement at elevated pressures up to 3 bar with a similar burner configuration where performed.

Laser-induced Incandescence

The laser-induced incandescence measurements were conducted with a Nd:Yag laser emitting at 1064 nm. The LII signal was detected at two different wavelengths around 400 nm and 700 nm using fast photomultipliers in combination with interference filters. Fluorescence of PAH´s is very unlikely to be induced, because of the low fluences and the high wavelength of the laser beam. Based on a LII model [1] accounting for absorption, conduction, sublimation, annealing, oxidation and radiation the particle sizes were derived.

Photoionization Mass Spectrometry

For MS measurements sample gas was drawn via a short quartz probe (50 cm, 6 mm id) equipped with a nozzle at its tip. The nozzle provided a pressure drop by a factor of about 60. The resulting drop together with short residence times of about 5 ms helped to minimize coagulation in the sampling line. Introduction to the MS was carried out via a pulsed valve. For photoionization a photon fluence of 3×10^5 W/cm² at a wavelength of 193 nm (ArF) was used. This ensures negligible fragmentation.

Results

The nanoparticle mass spectra show a bimodal behaviour in the HAB range covered, the lower mode with mean diameters between 2 and 3 nm (large circles), the upper mode around 5 nm (small circles) and more pronounced at larger heights. For LII only the upper mode is detectable (dots). In the overlapping region around Φ=1.9 a good match is found between LII and MS. Unfortunately, for larger Φ, that means higher masses, there is a cut-off in the MS mass range so that the high mode peak cannot be reliably measured. The low mode peaks, on the other hand, are observed throughout our stoichiometry range.

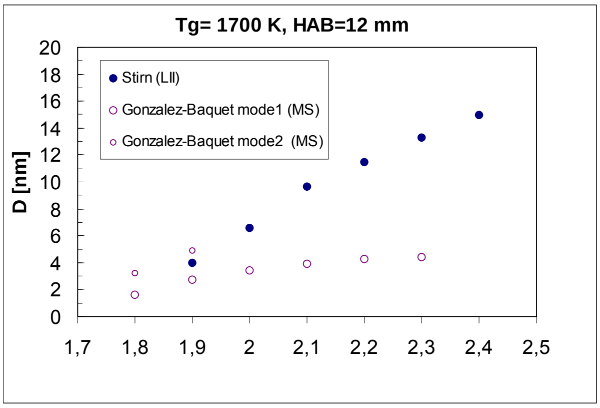

Fig. 1: Mean particle diameters of bimodal size distributions determined by mass spectrometry and laser-induced incandescence in a premixed ethylene air flame

Conclusion

We conclude that both methods show a complementary behaviour. Low mode sizes which are undetectable for LII are readily observable by MS. Conversely, at higher masses when the MS range tends to be limited, LII is particularly sensitive. In addition, it is obvious that for particles as small as 4 nm reliable data from LII can be extracted. MS has the potential to become a reliable sizing technique for small particles up to 10 nm provided the mass cut-off can be shifted to higher masses.

[1] H.A. Michelsen, Understanding and predicting the temporal response of laser-induced incandescence from carbonaceous particles, J. Chem. Phys. 118, 7012 (2003).

* Corresponding author: ronnie.stirn@dlr.de

Temperature measurements for LII evaluation in non-premixed flames – comparison between emission spectroscopy and CARS

M. Wendler*, G. Guevara, M.C. Weikl, R. Sommer, F. Beyrau, T. Seeger and A. Leipertz
Lehrstuhl für Technische Thermodynamik
Universität Erlangen-Nürnberg, Germany

The purpose of this work is to evaluate the accuracy of temperature measurements using emission spectroscopy in a parabolic flight set-up. The acquired time resolved temperature information is then used for particle sizing by TIRE-LII. For comparison, additional temperature measurements have been performed using coherent anti-Stokes Raman scattering (CARS).

Introduction

To study soot formation under microgravity conditions, TIRE-LII experiments have been performed during parabolic flight campaigns to simultaneously measure soot volume concentration as well as primary particle sizes in laminar non-premixed flames. As the temperature of the surrounding gas phase is an input parameter for primary particle size determination, it was necessary to measure this quantity at the same time. Thus, soot emission spectroscopy was chosen, as it is a robust measurement technique and rather simple to implement in an parabolic flight set-up. The applicability of this set-up was tested in the laboratory in comparison to CARS temperature measurements.

Experimental set-up

To evaluate the measurement procedure, data were taken in the same flame used in previous parabolic flight campaigns. The burner consists of two co-annular tubes (2.2 mm inner diameter, 30 mm outer diameter) for fuel and co-flow. The used gas flows (fuel: 75 scm^3/min ethylene, co-flow: 10 sl/min synthetic air) resulted in a non-premixed flame with a luminous flame length of 31 mm, and spectra were taken at several downstream positions from the burner exit.

Radial projections of light emitted by flame soot at a certain axial position is focused into the entrance slit of a spectrometer and detected by a CCD camera for wavelengths between 430 and 640 nm. Afterwards, the data were corrected for self-absorption using soot volume fraction data obtained by LII measurements, and an onion peeling algorithm for tomographic reconstruction is applied to obtain emission spectra at certain radial positions in the flame out of the projected data. Planck curves were fitted to the corrected spectra to get temperature profiles at certain axial flame position.

For accurate temperature determination coherent anti-Stokes Raman scattering with non-resonant background suppression was applied. C_2-interferences [1] were avoided by shifting the signal wavelength to an interference-free spectral region using a dual-pump CARS approach.

Results

Temperatures measured by emission spectroscopy and CARS show a rather good agreement at most of the examined downstream positions of the flame. For most flame heights the deviation between both techniques is smaller than 100 K. Thus, this method is suitable for temperature measurements in large part of the flame area. Unfortunately, it gives no reliable results in regions with very low soot concentration, especially at lower axial flame positions. Here, the use of a more sensitive camera could possibly lead to further improvements.

Acknowledgements

Parts of the work have been supported by the European Space Agency (ESA) and the German National Science Foundation (DFG)

[1] F. Beyrau, T. Seeger, A. Malarski and A. Leipertz, J. Raman Spectrosc., 34, 946–951 (2003).

* Corresponding author: monika.wendler@ltt.uni-erlangen.de

Pressure effects on LII-signals

A. Boiarciuc[1], F. Foucher[1], C. Mounaïm-Rousselle[1*]
[1]Laboratoire de Mécanique et d'Energétique
University of Orléans, France

Laser-Induced Incandescence of carbon black particles in relatively high-pressure conditions (1 to 30 bar) was studied. During the second part of the signal, laser-induced emission of carbon black is increasing with pressure, this being rather an unexpected trend. It is believed that the light emitted by laser-heated particles (even those situated outside the measurement volume) might be scattered by the particles inside measurement volume, this signal being recorded together with LII.

Introduction

Due to its advantages over other techniques Laser-Induced Incandescence (LII) was developed lately as a tool for real-time in-situ soot quantification. In many devices e.g. Diesel engines, combustion and soot formation occur in relatively high pressure conditions. Therefore, a particular attention should be paid to pressure effects on LII signals.

Laser-Induced Incandescence of carbon black in high-pressure conditions

An experimental facility was setup, the main feature being a pressure vessel containing carbon black particles. The particles are kept in suspension by means of a fan placed inside the vessel and the pressure is raised by means of an external air bottle. It is proven that temperature inside the vessel, measured with a thermocouple, changes only slightly with pressure (within 20 K for pressures up to 30 bar).

Particles are heated with the fundamental output of a Nd:YAG laser. LII signals are filtered through band pass filters at 441.6 and 650 nm, detected with two photomultipliers and recorded with 1 GHz sample rate, 8 bit acquisition system.

LII signals were recorded for pressures between 1 and 30 bar with an increment of 5 bar. LII evolution versus time for pressures in the investigated range is represented in Figure 1. The curves are normalized and averaged over 100.

As expected, higher pressures involve faster decay of LII signals during the first part of particles cooling. The differences in characteristic decay time as pressure increases are stronger for pressures between 1 and 10 bar, this feature was already observed by Hofmann et al. [1]. For pressures superior to 10 bar we observed that the decay time during the first part of LII signal changes only slightly.

During the second part of LII signals, an unexpected behavior was observed: the recorded signal increases as pressure raises. At this stage of the study, this trend is not completely understood. However, we assume that the incandescence emitted by particles including those outside the measurement volume might be scattered by particles located within the measurement volume (see reference [2]) and in the later part of LII signal scattering is stronger than incandescence. Moreover, enhanced agglomeration of particles is expected when raising pressure and so a stronger scattering signal, certainly in Mie regime, might be recorded together with LII.

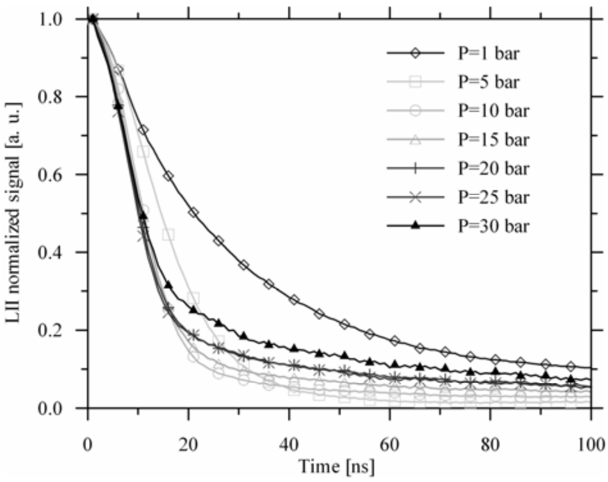

Fig. 1: LII normalized signals (averaged over 100)

Further work will be conducted in order to better explain the behavior of LII signals at relatively high pressures. Sampling of carbon black particles and TEM analysis will be the first step to clarify this behavior.

[1] M. Hofmann, W.G. Bessler, C. Schulz, H. Jander, Appl. Opt. 12, 2052 (2003)

[2] K.A. Thomson, D.R. Snelling, G.J. Smallwood, F. Liu, Appl. Phys. B 83, 469-475 (2006)

[3] B.F. Kock, T. Eckhardt, P. Roth, Proc. Combust. Inst. 29, 2775 (2002)

* Corresponding author: christine.mounaim@univ-orleans.fr

Effect of pressure on thermal accommodation coefficient

B.J. Stagg*
Columbian Chemicals Company
West Oak Commons Ct, Marietta, GA, USA

The thermal accommodation coefficient, α, for carbon black in air was measured for various sub-atmospheric pressure levels. Surprisingly, it was found that α is dependent upon pressure, increasing from ~0.1 at 1 atm. to ~0.5 at 0.18 atm.

Introduction

The thermal accommodation coefficient, α, is an important parameter in predicting the cooling rate of nano-sized particles in the free-molecular regime. Its value, which can theoretically range from 0 to 1, is critical in calculating particulate fineness from LII data. In the literature of LII modeling, reported values of α have varied widely, from a low value of 0.26 to a high value of 0.9 [1].

Experimental Details

LII measurements were performed on carbon black sampled from a process stream at a manufacturing plant. The sampling process dilutes and cools the stream, such that the LII measurements are performed on a stream of ambient temperature. For this particular set of experiments, the pressure in the optical cell was reduced to sub-atmospheric levels by "sucking" the aerosol stream through a small orifice using the vacuum generated by a venturi eductor. A diagram of the setup used is shown in Figure 1.

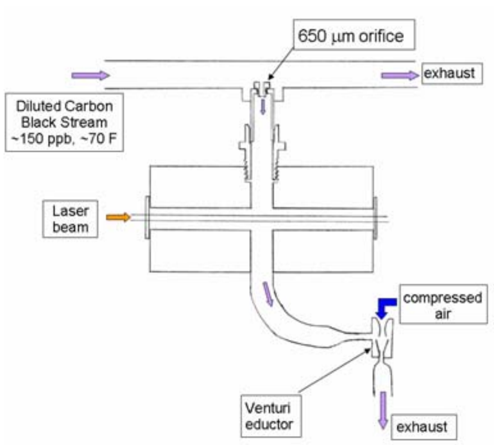

Fig. 1: Experimental Setup

Data Analysis and Results

In the free-molecular regime, the temperature decay rate measured with LII can be related to the particulate fineness as [2]

$$\frac{d}{dt}\left\{\ln\left(T_c - T_g\right)\right\}\Big|_{t=0} = -\frac{\theta}{D_{32}} \quad , \tag{1}$$

where T_c is the "effective" temperature of the polydisperse group of particles determined by LII measurements, D_{32} is the Sauter Mean Diameter of the particle distribution, and θ is given as

$$\theta = \frac{3\alpha\, p_g}{4\rho\, c_s T_g}\sqrt{\frac{8k_B T_g}{\pi\, m_g}}\left(\frac{\gamma^* + 1}{\gamma^* - 1}\right) \quad . \tag{2}$$

As seen from these equations, the measured temperature decay rate can be used to calculate either D_{32} or α, but not both simultaneously. For this series of measurements, a sample of the carbon black was collected for nitrogen adsorption measurements. The external surface area was found to be 91 m^2/g, giving an SMD value of D_{32} = 35.6 nm. With this value for SMD, the values of α calculated from LII are shown in Fig. 2, where it is seen that α has a value of ~0.1 at 1 atm. of pressure and increases to ~0.5 as pressure decreases to 0.18 atm.

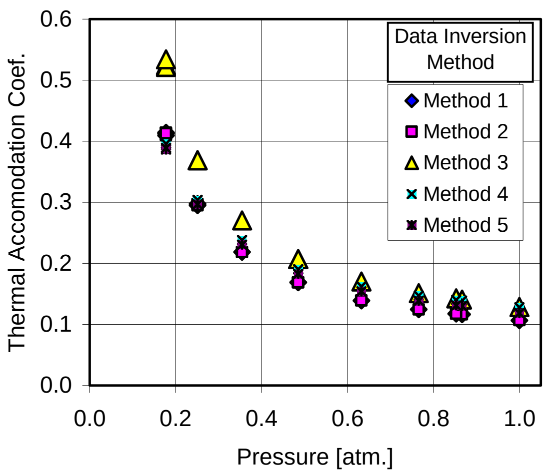

Fig. 2: Inferred α Values

[1] D. Snelling, F. Liu, G. Smallwood, O. Gulder, Combustion and Flame, 136, 180 (2004).
[2] F. Liu, B. J. Stagg, D. R. Snelling, G. J. Smallwood, IJHMT, 49, 777-788 (2006).

* Corresponding author: bstagg@columbianchemicals.com

Laser-induced incandescence for measuring soot particle emission from aero-gas turbines

J. Delhay[1], P. Desgroux[1*], E. Therssen[1], John Black[2],
[1]Physico-Chimie des Processus de Combustion et de l'Atmosphère (PC2A), UMR-CNRS
Université des Sciences et Technologies de Lille, Villeneuve D'ascq cedex, France
[2] Strategic Research Centre, Rolls Royce plc, Derby, UK

A compact device for measuring LII collected in the 'backward' direction, i.e. counter to the propagation of the laser, is described. This configuration is particularly well adapted to large scale practical application, such as in-situ soot volume fraction in aero-engine exhausts. Several tests were performed on different jet engines and we present results obtained on helicopter turbine within the framework of European project AEROTEST.

Set-up

The device presented in this paper, was developed during European projects (AEROJET 1 and 2) to measure the soot volume fraction in aero-engines in-situ. It is composed of a YAG laser pulsed at 10 Hz (Quantel CFR 400) at the fundamental wavelength (1064nm) to heat soot particles from their initial temperature to around 4000K. A rotating prism is used to scan the laser beam across the engine exhaust plume. The LII signal is collected through the same prism and diverted to an intensified CCD camera (PCO Dicam) using a dichroic mirror. Each element of this equipment is monitored via the same software developed in previous European projects.

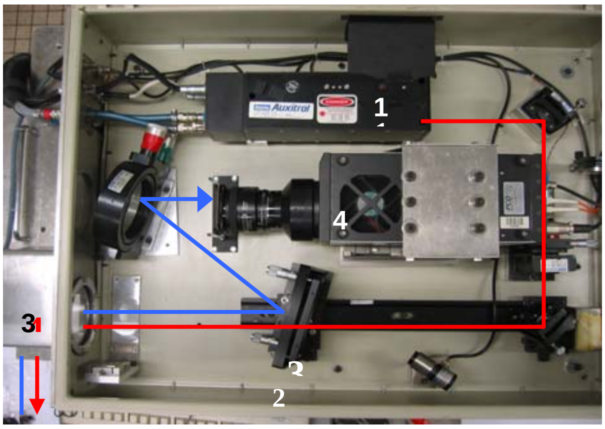

Fig. 1: Experimental set-up. (1) Nd/YAG laser; (2) dichroic mirror; (3) rotating prism; (4) Intensified CCD camera.

These elements are in a compact box and are easily transportable. A calibration procedure based on extinction is performed in a chimney where kerosene soot particles are produced by a 40 kW domestic burner. Application of the LII technique in the exhaust of a modified helicopter turbine demonstrates the sensitivity of this device for practical use for soot monitoring issued from aero-engines.

Measurements in helicopter turbine

Measurements were performed in a modified Rolls-Royce Gnome helicopter engine. Measurements were performed 1 cm downstream the cone of the turbine where the temperature of exhaust gases is around 620K at 20000 rpm. The exit diameter of the turbine is 28 cm.

Figure 2 shows the integrated LII signal from single laser pulse images taken during engine start up. The signal peaks on light-up and falls to a steady value after ~30 s. Similar behaviour has been observed on other engines elsewhere (*Jenkins [1]).*

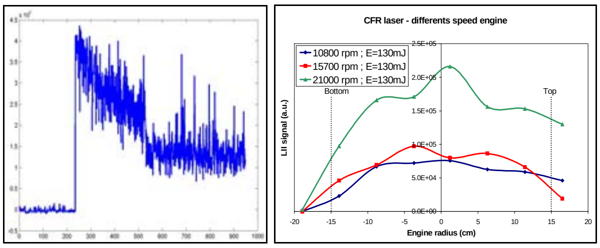

Fig. 2: start up of the turbine (at left) and signal recorded at 3 different engine speeds (at right).

The soot profile in exhaust gas was measured at different engine speeds. It is clearly visible that the quantity of soot increases with the engine speed.

Acknowledgements

This work is supported by Auxitrol S.A. and MEPACA (Pôle capteur, Conseil Regional Centre). The authors thank the European Community for financial support of this research under the 6th PCRDT, STREP 502856 AEROTEST. The authors thank P.E. Bengtsson and H. Bladh for fruitful collaboration within AEROTEST.

[1] Jenkins et al, AIAA 2002-0828, (2002).

* Corresponding author: pascale.desgroux@univ-lille1.fr

Two-color time-resolved LII study of iron oxide nanoparticle formation in a premixed flat low pressure flame

H. Dörr*, H. Bockhorn, and R. Suntz
Institut for Chemical Technology and Polymer Chemistry
University of Karlsruhe (TH), Germany

Two-color time-resolved laser induced incandecsence is evaluated with respect to metal oxide particle sizing in a low pressure premixed $H_2/O_2/Ar$ flame doped by iron pentacarbonyl. To influence the heat conduction/sublimation ratio the laser fluence and the height above burner are varied to determine the parameters of heat conduction and vaporization. Typically the decays of the LII signal occurred within 250ns. For comparison the iron oxide nanoparticles are characterized in-situ by particle mass spectrometry, elastic scattering, extinction measurements, ex-situ by TEM analysis and dynamic light scattering.

Introduction

The laser induced incandescence (LII) is quite well established for particle sizing of carbonaceous particles, typically of soot from various gas-phase processes [1]. Two-color time-resolved LII (2C-TR-LII) determines as pyrometric method directly the temperature evolution of the particles in the probe volume during the LII, avoiding some uncertainty in modeling the laser absorption. For non carbonaceous particles only very few studies are available. Significantly lower melting and vaporization temperatures, a small data basis of the relevant particle properties like e. g. heat conduction, accommodation coefficients, vaporization enthalpy, complicate the signal evaluation. Furthermore by the lower melting and vaporization points the particles cannot reach as high temperatures as soot particles, which with regard to Planck's law shifts the emitted radiation to the red with much smaller signal amplitudes. Additionally the temperature difference between the laser heated particles and particles within a reacting flow like a flame, becomes smaller, making particle formation and growth studies in a hot environment challenging.

Experimental

The versatile experimental setup with the applied laser diagnostics and the particle mass spectrometer is shown in figure 1:

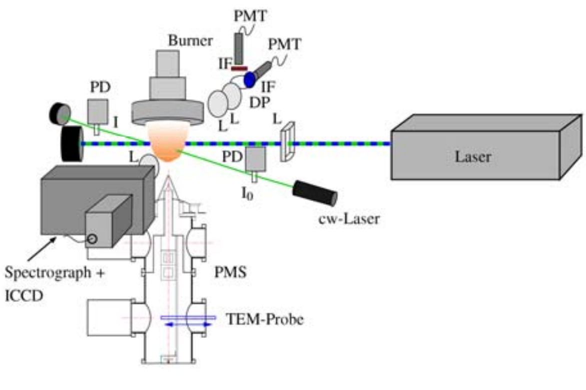

Fig. 1: Experimental setup

The formation and growth of iron oxide nanoparticles within a burner stabilized premixed flat low pressure $H_2/O_2/Ar$ flame doped by iron pentacarbonyl (approx. 2.5 Vol-‰) are studied in situ by 2C-TR-LII, elastic scattering, spectral analysis and extinction measurements as optical diagnostics. As further in situ particle diagnostics particle mass spectrometry [2] is applied. As ex situ methods molecular beam probed TEM samples and in various solvents dispersed powder samples were investigated by dynamic light scattering.

Preliminary results

Although the spectral analysis with the blue sensitive ICCD did not permit the observation of LII broadband emission, the LII signal can be recorded with good S/N ratio by two PMT and interference filters with $\Delta\lambda$(FWHM)=50nm as shown in figure 2.

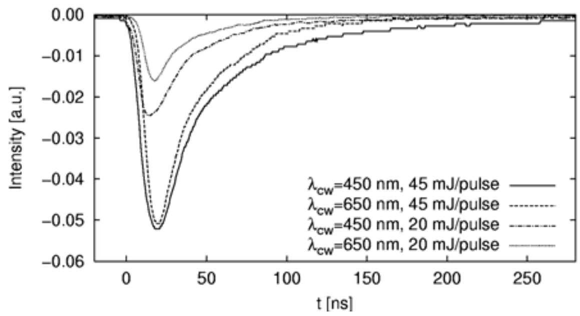

Fig. 2: Variation of laser flux density

The height resolved measurements indicates the applicability of particle sizing by 2C-TR-LII even in the hotter flame zones at lower height above burner values.

The data evaluation is based on modeling LII for various laser fluences to elucidate the first and second moment of a lognormal size distribution.

[1] C. Schulz, B.F. Kock, M. Hofmann, H. Michelsen, S. Will, B. Bougie, R. Suntz, G. Smallwood, Appl. Phys. B 83 (3), 333 (2006).

[2] H. Dörr, R. Suntz, and H. Bockhorn, VDI-Bericht 1839, 185 (2004)

*Corresponding author: doerr@ict.uni-karlsruhe.de

In-cylinder particulate sizing with combined TR-LII/2C pyrometry

B. Bougie[1,2], L.C. Ganippa[1,3], A.P. van Vliet[1], W.L. Meerts[1], N.J. Dam[1], J.J. ter Meulen[1]
[1]Applied Molecular Physics, Institute for Molecules and Materials, Radboud University Nijmegen, The Netherlands
[2]Current address: Multi-Scale Physics Delft University of Technology, Delft, The Netherlands
[3]Current address: School of Engineering and Design, Brunel University, London, UK

Time-resolved laser-induced incandescence (TR-LII) measurements have been performed inside the cylinder of a heavy-duty Diesel engine as a function of the crank angle, at two probe locations and for two engine loads. The TR-LII intensities have been recorded in two disjunct wavelength bands. Assuming a log-normal particle size distribution, an increase of the soot particle radius could be measured, followed by a decrease later on during the combustion cycle.

Introduction

This paper focuses on the determination of the soot particulate size distribution with TR-LII at different probe locations for different engine loads. The method is similar to the approach presented by Kock *et al.* [1]. Their model [2] is used to analyze the soot particulate sizes from the TR-LII measurements. The model incorporates cooling phenomena by conduction, sublimation and radiation. The ambient pressure is incorporated in the cooling contributions by conduction and sublimation. The assumption is that the particulates have a spherical shape. In the current study two-color pyrometry is used to measure the initial temperature of the soot particles immediately after the laser pulse.

Experimental setup

Experiments have been performed on the optically accessible cylinder of a heavy duty Diesel engine with a compression ratio of 15. A schematic picture of the setup is shown in Fig. 1. The laser beam (1064 nm, 0.25 J/cm^2) was guided top-down through the cylinder and the TR-LII traces have been recorded through the side-window. A portion of the LII is guided to an ICCD camera which is mounted on a spectrograph. The other part of the LII is filtered with a BG 18 filter, and focused on two photo-multiplier tubes (PMT), via a beam splitter. Each of the PMTs is equipped with its own filter in order to be able to measure the intensity ratio of both signals. A more elaborate description of the experimental setup can be found in [3,4].

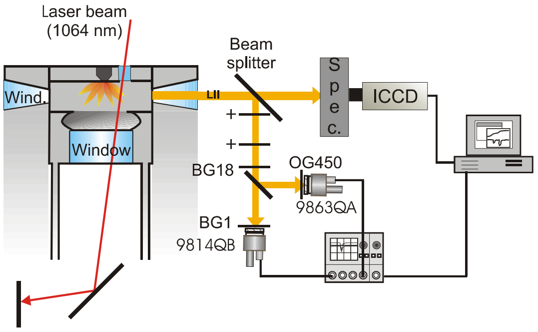

Fig. 1: Experimental setup

Results

TR-LII curves have been recorded for two engine loads (25% and 50%) at two probe locations. The measured curves are only interpreted as TR-LII if both on the camera connected to the spectrograph glowing soot is visible (Fig. 2) and on both PMTs a TR-LII curve is measured. For the analysis of the TR-LII curves, a Wiener deconvolution has been applied with the response function of the detection system of the PMTs, during which the power of the noise spectrum has been conserved [5]. During the complete combustion cycle, TR-LII curves are measured only infrequently. This is probably due to the small probe volume. On the poster the dependence of the particle size as a function of the engine load and probe location will be shown. Results for different engine loads and the dependence of the particle size as a function of the probe location are compared.

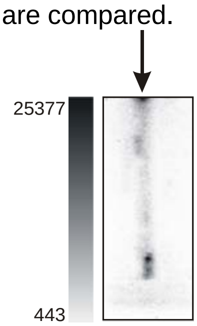

Fig. 2: Glowing soot present in the field of view. The grey scale is a measure for the LII intensity in a.u.

Acknowledgements

This work has been financially supported by the Technology Foundation STW, applied science division of NOW and the technology programme of the Dutch ministry of economic affairs.

[1] B.F. Kock, Th. Eckhardt, P. Roth, *Proc. Combust. Inst. 2002*, **29** (2) (2002), 2775-2781.
[2] B.F. Kock, P. Roth, *Proc. European Combustion Meeting*, (2003).
[3] B. Bougie, L.C. Ganippa, N.J. Dam, J.J. ter Meulen, *Appl. Phys. B: Lasers and Optics*, **83** (3) (2006), 477-485.
[4] B. Bougie, L.C. Ganippa, A.P. van Vliet, W.L. Meerts, N.J. Dam, J.J. ter Meulen, *Proc. Combust. Inst. 2006*, in press.
[5] B. Bougie, L.C. Ganippa, A.P. van Vliet, W.L. Meerts, N.J. Dam, J.J. ter Meulen, *Combustion and Flame*, **145** (3), 635-637.

Measuring accommodation coefficients using laser-induced incandescence

K. J. Daun*, G. J. Smallwood, F. Liu, and D. R. Snelling
National Research Council of Canada, Ottawa, Canada

This study presents thermal accommodation coefficients between soot and different gases. The dependence of these values on the molecular mass of the gas is investigated.

Introduction

Laser-induced incandescence has recently been used to measure thermal accommodation coefficients, α_T. Although most experiments carried out to date provide soot/air or soot/flame-gas accommodation coefficients, a recent study [1] presents α_T values between soot and four other gases. The present study expands this data to include more gases and explores the relationship between α_T and the molecular mass of the gas.

Theory

Although the physics of gas-surface interactions is highly complex and not fully understood, several phenomenological models accurately describe the dependence of α_T on different parameters, the most important being the ratio of the molecular mass of the gas and the atomic mass of the surface atoms, $\mu = m_g/m_a$. The earliest and most robust model was proposed by Baule [2, 3], who predicted α_T based on the kinetic energy transferred when a moving rigid sphere representing a gas molecule collides with a stationary rigid sphere representing a surface atom,

$$\alpha_T = \frac{2.4\mu}{(1+\mu)^2}. \qquad (1)$$

This model is physical only if $\mu < 1$, since the surface atom could not otherwise back-scatter the gas molecule. If $\mu > 1$, lattice forces between multiple surface atoms help repel incident gas molecules. Burke and Hollenback [4] suggest that m_a can be adjusted to account for these lattice forces.

Experimental Apparatus

Soot is extracted at a height of 52 mm above a Gülder burner operating at conditions described in [5], and is induced into a motive gas in the venturi section of a mini-eductor resulting in dilution ratios between 30:1 and 100:1. The mixture flows into a closed chamber where two-color laser-induced incandescence is carried out. The thermal accommodation coefficient is then calculated from the effective temperature time-decay following the procedure described in [5].

Results

Values of α_T between soot and different gases are plotted in Fig. 1. The accommodation coefficient increases with increasing m_g for monatomic gases as predicted by Baule theory, but decreases for diatomic gases. Figure 2 shows the monatomic gas data plotted with Eq. (1) assuming an effective atomic surface mass of 119 amu, determined by least-squares fit. Although the general trend of the data agrees with the Baule model, Eq. (1) is not a good fit to the data if m_s is constant. A better fit is found by letting m_s be a function of m_a, which is consistent with the theory proposed in [3]. Values of m_s were solved by fitting Eq. (1) to the experimentally-measured α_T values for monatomic gases, and were found to be a hyperbolic function of m_a, as shown in Fig. 2.

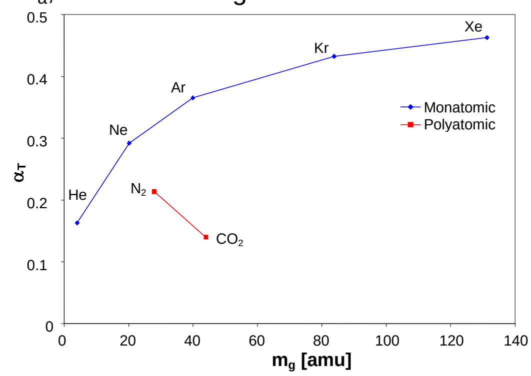

Fig. 1: Experimentally-determined values of α_T between soot and different gases.

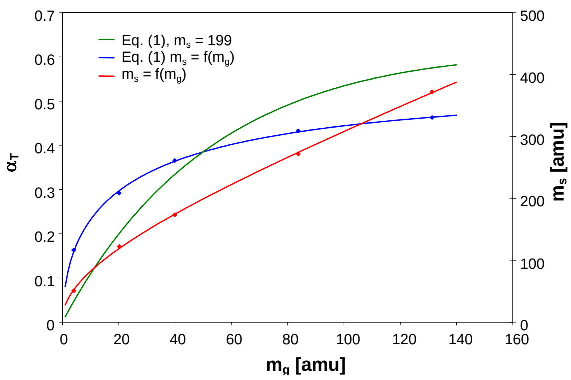

Fig. 2: Comparison of Baule theory to experimentally determined α_T values for monatomic gases.

[1] A. V. Eremin, E. V. Gurentsov, M. Hofmann, B. F. Kock, C. Schulz, App. Phys. B. 83, 449-454 (2006).
[2] B. Baule, Ann. Physik, 44, 145-176 (1914).
[3] F. O. Goodman, Surf. Sci., 3, 386-414 (1965).
[4] J. R. Burke, D. J., Hollenbach, Astrophysical J. 265, 223-234 (1983).
[5] D. R. Snelling, F. Liu, G. J. Smallwood, Ö. L. Gülder, Comb. and Flame, 136 180-190 (2004).

* Corresponding author: kyle.daun@nrc-cnrc.gc.ca
International Discussion Meeting and Workshop 2006: Laser-induced Incandescence, Quantitative interpretation, modelling, application

Comparison of TR-LII sizing for pure carbon and hydrogen-containing carbon particles

A. Eremin[1], M. Falchenko[1], E. Gurentsov[1*], B. Kock[2], R. Starke[2], C. Schulz[2]
[1]Institute for High Energy Density RAS, Moscow, Russia
[2]IVG, Universität Duisburg-Essen, Duisburg, Germany

Time-Resolved LII (TR-LII) particle sizing was performed for the pure carbon particles and for the particles holding some amount of hydrogen. These particles were formed from supersaturated carbon vapor and from carbon vapor with the addition of hydrogen atoms, by the laser photolysis of C_3O_2 or C_3O_2+H_2S. The current particle sizes were measured by TR-LII, while the final count median diameter of particles and the particle size distribution were analyzed by Transmission Electron Microscopy (TEM). The value of thermal accommodation coefficient for argon at the carbon-hydrogen particle surface was extracted by the comparison of TR-LII particle sizing with the TEM data and was found to be 0.3.

Introduction

The aim of this work is to study the influence of hydrogen on the formation of carbon particles. In previous work [1] the carbon particle formation was investigated during pure carbon vapor condensation at room temperature. Here, we analyze the influence of hydrogen atoms on carbon vapor on condensed particle properties using TR-LII and TEM.

Experimental

The method of laser-induced photo-dissociation of C_3O_2 [1] with addition of H_2S was applied as a source of carbon and hydrogen atoms for the study of particle formation. A quartz cell (10×10×5 mm) was evacuated and filled with 10 mbar C_3O_2 + 1 mbar H_2S diluted by Ar at pressure of 1 bar. The photo-dissociation of this mixture leads to the generation of 1 mbar C and 0.4 mbar H. Additionally, 0.4 mbar HS, 2 mbar CO and 9 mbar C_3O_3 remained in the mixture as impurities.

The equipment for TR-LII measurements consisted of a pulsed Nd:YAG laser (1064 nm), two photo-multipliers for the detection of particle emission at 694 and 550 nm. LII signals were evaluated using a updated Melton model included the changing heat capacity of carbon with temperature, particle-size distribution, and particle evaporation. The material properties of conventional soot were used for data analysis. The thermal energy-accommodation coefficient α for pure carbon particles was taken 0.44 in accordance to [1].

The particle samples of pure carbon particles and particles with addition of hydrogen were analyzed by TEM. Assuming a log-normal particle-size distribution, the count median diameter (CMD) and the standard deviation σ of final particles were extracted from the TEM micrographs and were found to be CMD = 11.5; σ = 1.3 for the pure carbon particles (a good agreement with [1]) and CMD = 9; σ = 1.2 for the hydrogen-containing particles.

Results

Figure 1 shows the observed temporal variation of particle sizes for pure carbon hydrogen-containing carbon particles. A difference between the final LII and the TEM sizes was found for the hydrogen-containing particles, which was attributed to the variations in thermal energy-accommodation coefficient due to different properties of the particle surfaces. Thus, the value of α for the hydrogen-containing particles was found to be 0.3, i.e. close to soot data (0.23 – 0.38) [2].

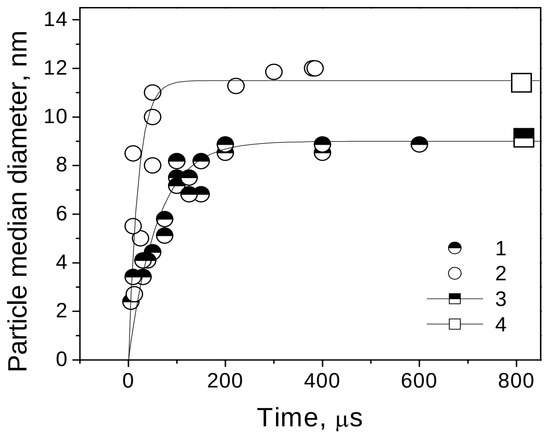

Fig. 1: Carbon and hydrogen/carbon nanoparticle growth in Ar. 1,3 – data for hydrogen-containing particles; 2,4 – data for pure carbon particles; 1,2 – TR-LII data; 3,4 – TEM data.

[1] Eremin A.V., Gurentsov E.V., Hofmann M., Kock B.F., Schulz C. TR-LII for sizing of carbon particles forming at room temperature, Appl. Phys. B, 83, 449-454 (2006).

[2] Snelling D.R., Liu F., Smallwood G.J. and Gülder Ö.L., Combust. Flame, 136, 180-190 (2004).

* Corresponding author: gurentsov@ihed.ras.ru

LII in a high vacuum and up date and LII in carbon black from a particle generator

V. Beyer[1] *and D. A. Greenhalgh*[1]*,*
D. Clavel[2]*, K. Daun*[2]*, F. Liu*[2]*, B. Sawchuck*[2]*, G. Smallwood*[2]*, D. Snelling*[2] *and K. Thomson*[2]
[1]School of Engineering Cranfield University
[2]National Research Council of Canada, Ottawa, Canada

LII in a high vacuum was first studied in detail last year and some preliminary findings were given at the LII workshop in Duisburg (2005) and subsequently published in a special issue of Applied Physics. This paper gives a brief up-date of this work and includes further detailed analysis of the experimental results. Further details on the estimates of E(m) has been made using a highly accurate NRC LII system. The results suggest that aggregation and agglomeration can be important.

We have performed LII measurement on carbon black agglomerates generated using by dispersing polarised carbon black in water and then promptly evaporating a fine aerosol mist. The generated carbon black agglomerates have been characterised by TEM. We have estimated E(m) from heating and also shown an apparent variation of both soot volume fraction and estimates of primary particle size with fluence. We believe the results to be consistent with break-up of the agglomerates which is enhanced by fluence.

Particle size measurements with two color TIRE-LII

R. Hadef[1*], R. Stirn[2], KP. Geigle[2], M. Aigner[2]
[1]Institut de Génie Mécanique, Université Larbi Ben M'Hidi, Oum El Bouaghi, Algérie
[2] Institut für Verbrennungstechnik, DLR, Stuttgart, Germany

Two-color TIRE-LII was applied for the sizing of soot particles. The experiments were performed in a premixed ethylene/air flame burning on a sintered stainless steel plug (McKenna) burner with equivalence ratios (ϕ) of 2.0 to 2.6 at a height above the burner of 12 mm. The flame was stabilized with a 20 mm thick steel plate with a diameter of 60 mm which was fixed 21 mm above the burner surface (HAB).

Introduction

The aim of this investigation is to more assess the performance of the LII model by comparing the results obtained simultaneously at two different detection wavelengths. The data will be useful for the further development of soot-formation model.

LII Model and Experiments

The LII model described in Ref. [1] was used in this study by adjusting the mass accommodation coefficient α_M from 0.8 to the value of 0.5 [2] in addition to the assumption of a constant value (0.261) for the refractive index absorption function *E(m)* [3]. We have validated this model with the experimental measurements of time resolved LII in a laminar ethene diffusion flame obtained at several laser fluences [4], see Fig. 1.

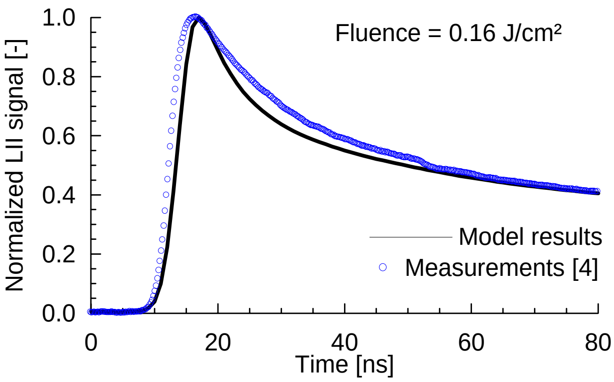

Fig. 1: LII signal for a 35-nm particle at 1900 K.

Results

The LII signal excited by a single Nd:YAG laser pulse (1064 nm, 0.11 J/cm^2) is observed at two detection wavelengths: 400±8nm and 700±21nm. For either measurement, 300 signals were averaged in order to reduce noise, and an average signal without laser irradiance was subtracted in order to account for the natural flame luminosity. Normalized model LII signals over the complete temporal range for different initial particle diameters are fitted to the measured one until the best fit is attained. An example of the measured LII signal fitted to the calculated signal is shown in Fig. 2.

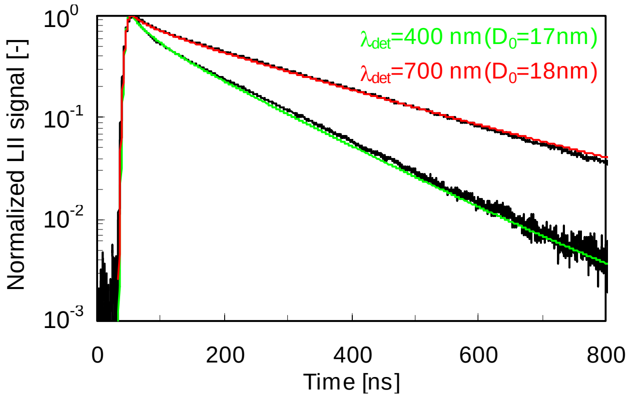

Fig. 2: Normalized LII signal as function of time, Experiment (ϕ=2.30) and calculated for T_g=1700 K, at two different detection wavelengths.

Fig. 3 shows that the obtained sizes at two different detection wavelengths are nearly identical.

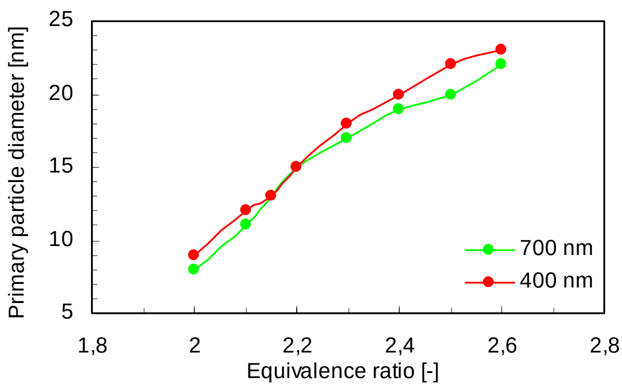

Fig. 3: Soot particle size measured by TIRE-LII as a function of ϕ at 12 mm HAB in the flame.

[1] R. Hadef, V., Krüger, K.P. Geigle, M. S. Tsurikov, Y. Schneider-Kühnle and M. Aigner, Oil & Gas Science and Technology 61 in press (2006).

[2] V. Philipps, E. Vietzke, and K. Flaskamp, Surf. Sci. 178, 806–812 (1986).

[3] D. R. Snelling, K. A. Thomson, G. J. Smallwood, Ö. L. Gülder, E. J. Weckman and R. A. Fraser, AIAA Journal 40, 1789-1795 (2002).

[4] H. A. Michelsen, P. O. Witze, D. Kayes and S. Hochgreb, App. Optics 42, 5577-5590 (2003).

* Corresponding author: rhadef@rocketmail.com

A web-based interface for modeling laser-induced incandescence (LIISim)

M. Hofmann*, B.F. Kock, C. Schulz,
IVG, Universität Duisburg-Essen, Duisburg, Germany

In this study we present a model for laser-induced incandescence (LII). Different heat conduction models can be selected and mono- or poly-disperse particles can be chosen as well as isolated, single particles or aggregates. We present a web interface that allows the scientific community to directly use this model. This will simplify the comparison of LII models developed by different research groups.

Introduction

Laser-induced incandescence (LII) has emerged as a useful tool to measure volume fractions and sizes of particles in the sub-micron region. The determination of particle sizes relies strongly on the use of models that accurately describe the micro-physical mechanisms of particle heating and cooling. However, recent comparisons have shown that large discrepancies exist between different approaches [1]. The motivation for the present study was to develop a model for LII that includes the recent advancements in the theoretical understanding of LII and to make it available to the scientific community by a web interface. This will simplify the comparison of different models and reveal deficiencies in the underlying sub models.

Heat and mass transfer in modeling LII

The basis for "LIISim" is the energy and mass balance of a single spherical particle including the absorption of laser energy and heat loss due to vaporization, heat conduction, radiation and change in internal energy.

The change of internal energy is given by $d(m_p c_p T_p)/dt$ [2]. Here, m_p is the particle mass, c_p the particle heat capacity, T_p the particle temperature and t the time. It should be noted that most models use the expression $m_p c_p dT_p/dt$ for the change in internal energy. This expression ignores the change in internal energy due to the temperature dependence of the particle's heat capacity which can have a significant influence on the temperature decay.

The expressions used for vaporization in the transition regime are given in [3].

Different heat conduction regimes can be selected when running the model: The free molecular regime, the continuum regime and the transition regime. In the latter case, the heat conduction model of McCoy and Cha [4] or Fuchs [5] can be used. In this way, the model can be applied to any Knudsen condition, i.e. low, atmospheric and high pressure.

Particles can be chosen to be mono-disperse or poly-disperse, following a lognormal distribution.

The effect of aggregation of primary particles on the heat conduction has been taken into account as described by Liu et al. [6]. The effects of aggregates on the evaporation term are neglected and aggregates should be only considered if the laser fluence is below the vaporization threshold.

The web interface

The web interface for LIISim is available at http://www.liisim.com. It enables the user to choose between different general settings for solving the energy- and mass balance, e.g. particle-size distribution, heat-conduction model and aggregate sizes. Parameters for the absorption of laser radiation can be set as well as for particle and gas-phase properties, e.g. particle diameter, gas pressure and energy accommodation coefficient. The values entered by the user are read in by a perl script which generates the input files for the LIISim executable. Solving the energy- and mass balance with a fourth order Runge-Kutta algorithm with the user-specified settings results in a new frame that shows a graph of the calculated LII signal as well as a link to the corresponding data file. In the data file, the time histories of the LII signal, the particle temperature, the particle diameter as well as the contributions of the different heat-loss mechanisms are listed. In this way, users can compare the LIISim results with own model predictions.

[1] C. Schulz, B.F. Kock, M. Hofmann, H. Michelsen, S. Will, B. Bougie, R. Suntz, G. Smallwood: Applied Physics B: Lasers and Optics **83**, 333 (2006)

[2] B.F. Kock, P. Roth: *Two-color TR-LII applied to in-cylinder Diesel particle sizing* (Proc. of the European Combustion Meeting, Orléans, 2003)

[3] G.J. Smallwood, D.R. Snelling, F. Liu, Ö.L. Gülder: J. Heat Transfer **123**, 814 (2001)

[4] B.J. McCoy, C.Y. Cha: Chem. Eng. Science **29**, 381 (1974)

[5] A.V. Filippov, D.E. Rosner: Int. J. Heat and Mass Transfer **43**, 127 (2000)

[6] F. Liu, M. Yang, F.A. Hill, D.R. Snelling, G.J. Smallwood: Applied Physics B: Lasers and Optics **83**, 383 (2006)

* Corresponding author: maximilian.hofmann@uni-due.de
International Discussion Meeting and Workshop 2006: Laser-induced Incandescence, Quantitative interpretation, modelling, application

Effects of soot absorption and scattering on LII intensities in a laminar coflow ethylene/air diffusion flame

F. Liu*, K. A. Thomson, G. J. Smallwood
Institute for Chemical Process and Environmental Technology
National Research Council, Canada

A 3D radiation model in absorbing, emitting, and scattering media is presented to quantify the effects of absorption and scattering by soot particle present between the measurement volume and the detector.

Introduction

Detected LII signals in reality rarely reflect the *true* radiation intensities emitted by laser heated hot particles in the laser probe volume due to the presence of other particles between the probe volume and the detector, Fig.1. The particles in the path between the probe volume and the detector play two roles. On one hand, they attenuate the emission intensity through absorption and out-scattering. On the other hand, they enhance the radiation intensity in the direction towards the detector through emission and in-scattering. The degree of LII signal modification depends on several factors such as the concentration and radiative properties of the other particles at the detection wavelength.

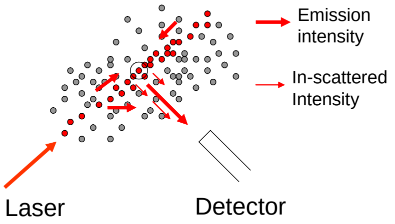

Fig. 1: A schematic illustrating the dual role of particles along the path between the laser probe volume and the detector.

It is important to gain quantitative understanding on the effects of particle absorption and scattering on the detected LII intensities. Such knowledge can be directly useful for improving the accuracy of particle temperature determined by two-color LII. Consequently, it helps improve the accuracy of LII based techniques for measurements of soot volume fraction, determination of soot absorption function E(m), and thermal accommodation coefficient.

Model and Method

We only concern the radiation intensity field at a moment near the end of the laser pulse when all the particles along the laser beam are heated to the same temperature. The radiation intensity is governed by the spectral radiative transfer equation

$$\xi\frac{\partial I_\lambda}{\partial x}+\eta\frac{\partial I_\lambda}{\partial x}+\mu\frac{\partial I_\lambda}{\partial x}=-(\kappa_{a\lambda}+\kappa_{s\lambda})I_\lambda+\kappa_{a\lambda}I_{b\lambda} + \frac{\kappa_{s\lambda}}{4\pi}\int_{\Omega'=4\pi}\Phi(\Omega'\to\Omega)I_\lambda(\Omega')d\Omega' \quad (1)$$

The radiative properties of polydisperse fractal soot aggregates are evaluated using the Rayleigh-Derby-Gans theory for polydisperse fractal aggregates (RDG-PFA). The scattering phase function is approximated by using the Henyey-Greenstein expression. The 3D spectral RTE is solved in cartesian coordinates using the discrete-ordinates method (DOM). To obtain the radiation intensity along an arbitrary direction, the DOS+ISW technique is employed.

Calculations were conducted in a laminar coflow ethylene/air diffusion flame with the distributions of soot volume fraction and temperature from experimental measured. To simulate the effect of the laser pulse, particles within 1 mm (simulating a laser beam about 2 mm) from the cord passing through z = 42 mm are assigned a temperature of 3600 K. Radiation intensities perpendicular to the laser beam were calculated. Table 1 summarizes the effects of absorption and scattering on the LII intensities at 400 nm and 780 nm detected horizontally at a height of z = 42 mm and passing through the flame centreline.

Table 1: Samples LII intensities at a selected detector location (in W/m^2 m ster)

	400 nm	780 nm
With scattering[a]	5.3136E10	9.8237E10
No scattering[b]	5.4495E10	9.8449E10
No in-scattering[c]	4.9635E10	9.7541E10
Emission only[d]	6.0265E10	1.0110E11

[a]Full simulation. [b]Scattering coefficient is set to 0.
[c]The in-scattering term in Eq.(1) is removed.
[d]Scattering coeff. is set to 0 and absorption coefficient outside the laser beam is also set to 0.

Scattering has stronger influence on the intensity at 400 nm. Further, attenuation is higher at 400 nm. Absorption and scattering clearly affect the ratio of the two LII intensities and thus the two-color LII particle temperature if no proper correction is made to the detected intensities.

Conclusions

A 3D radiation model was developed to quantify the effects of soot absorption and scattering on the detected LII intensities. Results of sample calculations in a laminar diffusion flame confirm that such effects are nontrivial and further studies are required.

* Corresponding author: fengshan.liu@nrc-cnrc.gc.ca
International Discussion Meeting and Workshop 2006: Laser-induced Incandescence, Quantitative interpretation, modelling, application

Time-resolved laser-induced incandescence (TIRE-LII) coupled with spectral emission measurements for particle sizing in high-pressure diesel combustion environments

R. Ryser, T. Gerber, T. Dreier*
Paul Scherrer Institute, Department of General Energy, Reaction Analysis Group,
Villigen PSI, Switzerland

Diesel engine combustion faces increased emission regulation standards worldwide with respect to the amount and size of soot particles escaping through the tailpipe. For efficient reduction of particulate emissions a better understanding of in-cylinder soot formation and destruction mechanisms is desirable. Laser-induced incandescence (LII) [1] is a non-intrusive optical technique for the *in-situ* characterisation of soot, such as mean particle size or spatial distribution of volume fraction. In this technique particulate matter is heated to high temperatures via absorption of a pulsed laser beam with fluence high enough to cause incandescence radiation to be recorded by one- or two-dimensional detectors. In time-resolved (TIRE) LII the soot particle size distribution is deduced from fitting an appropriate model function to the recorded transient signal intensity right after laser heat-up as derived from the particle energy and mass balance equations [2,3]. To accomplish this, in addition to a best knowledge of experimental parameters, i.e., laser fluence, beam profile, detection window, etc., an appropriate physical model for the description of the laser induced particle heating, evaporation and its subsequent cooling is necessary.

The present work describes the optically accessible high pressure Diesel spray combustion chamber at PSI for the simultaneous measurement of TIRE-LII signal traces at two separate detection wavelengths as well as of the spatially and spectrally resolved soot emission using an intensified CCD camera coupled to a spectrometer. Information on the mean soot particle size is evaluated by least squares fitting an appropriate physical model function adapted for the probed high pressure combustion environment [4] with known experimental parameters, such as gas pressure, spatially averaged particle temperature, laser fluence, etc. The submodel assumes a log-normal particle size distribution function and calculates temporal profiles of particle temperature and mean diameter as well as the LII signal intensity for a range of laser intensities representtative for the cross section of a Gaussian spatial beam in the measurement volume.

In the experiments, at initial gas pressures and temperatures (before ignition) between 0.5 and 4 MPa, and 773 K, respectively, and fuel injection pressures of 50 and 100 MPa soot is heated with the fundamental output of a Nd:YAG-laser (1064 nm, 10 ns pulse width) at pulse energies between 20 and 50 mJ. Laser-induced incandescence is collimated, separated by a dichroic beam splitter and focused on 2 photomultiplier tubes equipped with 460 and 630 nm interference filters, respectively. Both detector outputs are digitized on a fast storage oscilloscope (500 MHz bandwidth). Simultaneously, through a second observation window the laser- or flame-induced soot radiation along a vertical line is recorded at the exit plane of a grating spectrometer (focal length 300 mm) using an intensified CCD camera. After calibrating the detection system with a calibration source of known spectral radiance the 2-color LII signal profiles were evaluated for an effective soot particle temperature used as an experimental parameter in the subsequent fitting procedure.

We show that even at the pressures typical for these experiments TIRE-LII signal decays still can be temporally resolved with the present detection systems. Trends of the deduced particle size parameters with external gas and fuel injection pressure, temperature or residence time are discussed. The effects of unknown thermo-physical parameters and of mechanistic assumptions in the LII submodel on the extracted particle size parameters are investigated.

[1] T. Ni, J. A. Pinson, S. Gupta, R. J. Santoro: Appl. Opt. **34**, 7083 (1995)
[2] L. A. Melton: Appl. Opt. **23**, 2201 (1984)
[3] P. Roth, A. V. Filippov: J. Aerosol Sci. **27**, 95 (1996)
[4] B. F. Kock, T. Eckhardt, P. Roth: Proc. Combust. Inst. **29**, 2778 (2002)

* Corresponding author: thomas.dreier@psi.ch
International Discussion Meeting and Workshop 2006: Laser-induced Incandescence, Quantitative interpretation, modelling, application

Absolute intensity calibration of LII detectors

K. A. Thomson, D. R. Snelling, G. J. Smallwood
Institute for Chemical Process and Environmental Technology
National Research Council, Canada

Absolute intensity calibration is an integral component of auto-compensating laser induced incandescence (AC-LII) and other two-colour LII methods. Three sources: a tungsten strip filament, an irradiance standard with a calibrated reflector, and a lamp coupled with an integrating sphere, are compared. Differences between sphere and filament are below 10%. The irradiance standard differs by 30%. The integrating sphere is the preferred standard for excellent output uniformity (< 1 % deviation) across a large field-of-view, high intensity, good intensity control, and minimum indirect radiation bias.

Introduction

AC-LII is a valuable tool for the determination of soot concentration and effective particle diameter for soot aerosols in a variety of settings [1]. The method does not require calibration of the LII signal using a soot aerosol of known concentration; however, an absolute light intensity calibration of the LII apparatus is required. Several intensity calibration standards are commercially available. A comparison of three standards is presented.

Apparatus

The centre portion of the filament (i.e. 1 mm diameter) of a tungsten strip filament lamp is approximately invariant (< 10% variation) and can be used to calibrate LII systems which sample a small field-of-view. The lamp is small and fits various experimental setups (e.g. pressure vessels). The lamp used here was calibrated at NRC for brightness temperature (T_b) as a function of lamp current. Spectral radiance can be calculated from T_b using Planck function and the emissivity of tungsten. Commercial lamps are available.

Irradiance standards are lamps for which the spectral irradiance at a set distance from the bulb is uniform and known. The spectral radiance off a highly reflective (>98%) diffuse reflector located at this distance can be calculated. The reflector can be various sizes (e.g. 25 mm dia.); however, must face normal to the irradiance source. Therefore it cannot be normal to the detector. This does not impact the radiance observed by the detector provided the collection optic has a good depth-of-field. The radiance from the reflector is of fixed intensity and is weak against the background of stray emission from the intense irradiance standard (200 W bulb). Indirect radiation bias can be a problem.

The lamp and integrating sphere uses a bulb coupled to a highly reflective sphere. The spectral radiance of light emitted from a port on the side of the sphere (35 mm diameter here) is spatially uniform (< 1 % variation) and can be varied in intensity using a shutter. The spectral output is monitored by a spectrometer coupled to a second port on the sphere. Thus variation in intensity due to the shutter position or lamp aging is accounted for.

The experiment layout is shown in Fig. 1. The radiant emission from the measurement field-of-view (1 mm^2) was imaged onto a fiber optic (1:1) coupled to a de-multiplexer and two PMTs (Hamamatsu H5783-03 bialkali photosensor and H5783-20 photosensor) filtered for 445 and 783 nm. A light chopper modulated the light.

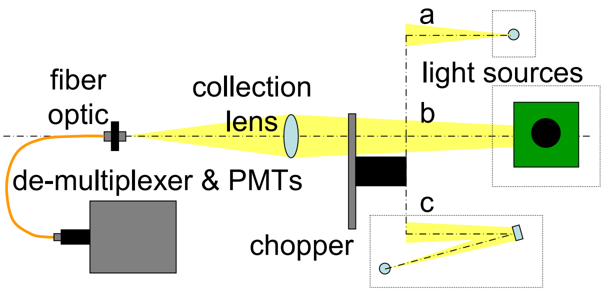

Figure 1: Calibration setup a.) strip filament lamp, b.) integrating sphere, and c.) irradiance standard

Table 1 includes the measured calibration factors. The filament and sphere standards agree to within 10%. The irradiance standard differs more significantly. It is postulated that the lamp has aged since purchase and a new lamp is on order.

Table 1: Calibration Factors [W/m^3 ster V]

λ	Filament	Irradiance	Sphere
445 nm	7.52e9	1.05e10	8.21e9
783 nm	1.67e12	2.00e10	1.52e12

The filament and sphere sources are easier to implement since the source sits in the location of LII measurement. The strength of the radiant emission is much stronger than that from an irradiated reflector and they face the detector normally. The sphere provides a large uniform source and lamp aging is internally account for; however, this assumes no drift of the lamp spectrometer. It is our opinion that the lamp coupled to an integrating sphere is the optimal light source for detector absolute intensity calibration. Future work will involve testing the source calibrations with help from the National Institute for Measurement Standards.

[1] D. R. Snelling et al., Appl. Opt. v44, p6773-6785, (2005).

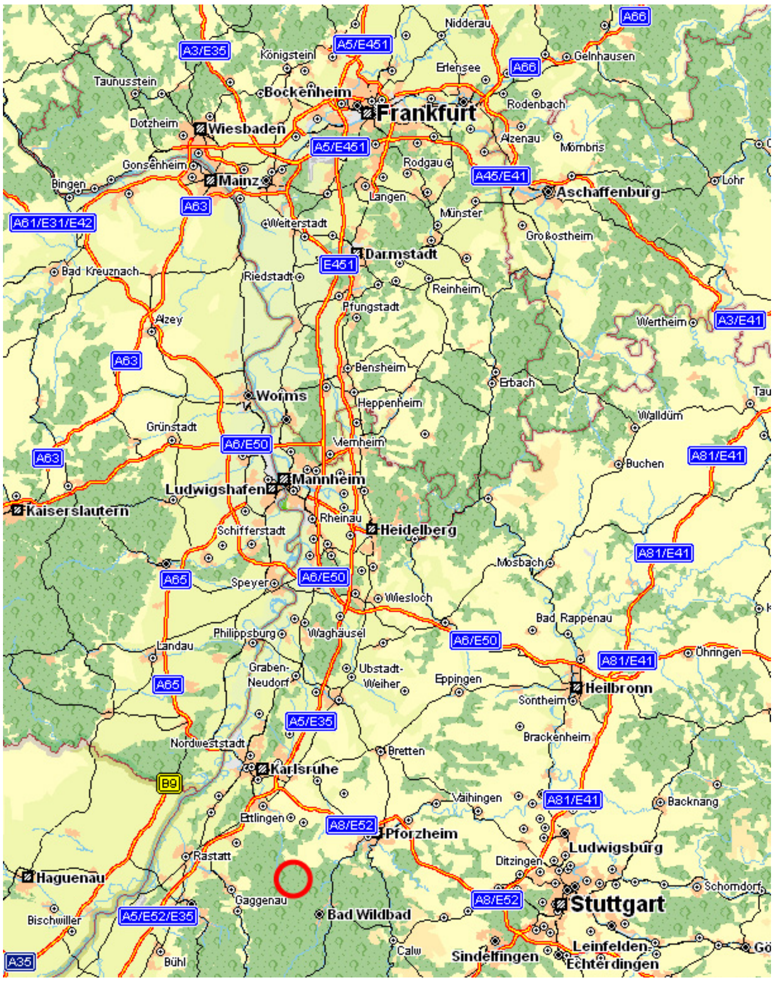
Frankfurt
Wiesbaden
Mainz
Darmstadt
Worms
Mannheim
Ludwigshafen
Heidelberg
Kaiserslautern
Heilbronn
Karlsruhe
Pforzheim
Stuttgart
Ludwigsburg
Haguenau
Bad Wildbad
Aschaffenburg

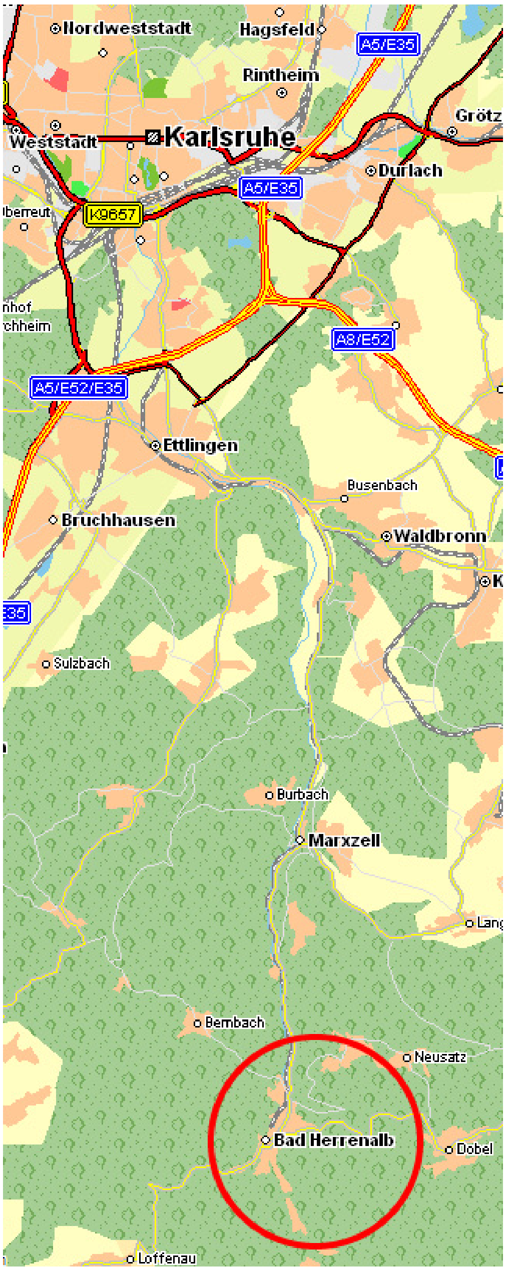
Nordweststadt
Hagsfeld
Rintheim
Karlsruhe
Weststadt
Durlach
A5/E35
K9657
A8/E52
A5/E52/E35
Ettlingen
Busenbach
Bruchhausen
Waldbronn
Sulzbach
Burbach
Marxzell
Bernbach
Neusatz
Bad Herrenalb
Dobel
Loffenau

2nd International Meeting and Workshop on

Laser-induced incandescence:
Quantitative interpretation, modelling, application

August 2-4, 2006 - Bad Herrenalb

University of Karlsruhe, Germany
Institut für Technische Chemie und Polymerchemie

Basic informations

Haus der Kirche

Haus der Kirche - Evangelische Akademie Baden
Dobler Str. 51, 76332 Bad Herrenalb
Deutschland
Telefon (07083) 928-0,
Fax (07083) 928-601
Email: haus@ev-akademie-baden.de